Published for SISSA by Springer

Received: *March 31, 2025*
Revised: *April 21, 2025*
Accepted: *May 5, 2025*
Published: *June 11, 2025*

Updated model-independent measurement of the strong-phase differences between D^0 and $\bar{D}^0 \to K^0_{S/L}\pi^+\pi^-$ decays

The BESIII collaboration

E-mail: besiii-publications@ihep.ac.cn

Abstract: The strong-phase differences between $D^0 \to K^0_{S(L)}\pi^+\pi^-$ and $\bar{D}^0 \to K^0_{S(L)}\pi^+\pi^-$ decays are one of the most important inputs in measuring the *CP* violating angle γ via $B^- \to DK^-$ decays. They also play a key role in studies of charm mixing and indirect *CP* violation. In this paper, the strong-phase differences are determined in a model-independent way with quantum-correlated D^0-$\bar{D}^0$ decays from $7.93\,\text{fb}^{-1}$ of e^+e^- annihilation data at $\sqrt{s} = 3.773\,\text{GeV}$ by the BESIII experiment. These results are the most precise to date and are expected to significantly reduce associated uncertainties in determining the *CP* violating angle γ and related charm mixing parameters.

Keywords: Charm Physics, e^+-e^- Experiments, Flavour Physics, CKM Angle Gamma

ArXiv ePrint: 2503.22126

https://doi.org/10.1007/JHEP06(2025)086

JHEP06(2025)086

Contents

1 Introduction

In the Standard Model (SM), *CP* violation in the quark sector is only attributed to the complex phase in the Cabibbo-Kobayashi-Maskawa (CKM) matrix [1, 2]. The unitarity nature of the CKM matrix permits its geometric representation as the Unitary Triangle (UT) in the complex plane. Specifically, the *CP* violating angle $\gamma = \arg(-V_{us}V_{ub}^*/V_{cs}V_{cb}^*)$ in the UT can be directly measured in the tree-level decays. These decays are expected to have negligible theoretical uncertainty [3]. The γ angle can also be indirectly inferred from the information of other CKM matrix elements [4], which are more susceptible to new physics effects. Hence, the direct measurements of γ provide a stringent test of the CKM matrix unitarity and a potential avenue in the search for new physics beyond the SM [5].

JHEP06(2025)086

The leading decay channel for the direct measurement of the angle γ is $B^{\pm} \to DK^{\pm}$, $D \to K^0_S\pi^+\pi^-$ [6], where D represents a superposition of D^0 and $\bar{D}^0$. The amplitude of the B^- decay is written as

$$f_B(m^2_+, m^2_-) \propto f_{D^0}(m^2_+, m^2_-) + r_B e^{i(\delta_B-\gamma)} f_{\bar{D}^0}(m^2_+, m^2_-). \tag{1.1}$$

Here, $m^2_{\pm}$ is the squared mass of $K^0_S\pi^{\pm}$, $f_{D^0/\bar{D}^0}(m^2_+, m^2_-)$ denotes the amplitudes of the $D^0/\bar{D}^0 \to K^0_S\pi^+\pi^-$ decays, δ_B is the strong-phase difference between the color-favoured and color-suppressed amplitudes of $B^{\pm} \to DK^{\pm}$, and r_B is the modulus of the suppressed to favoured amplitudes. The amplitude of the $D^0 \to K^0_S\pi^+\pi^-$ decay $f_{D^0}(m^2_+, m^2_-)$ is described by the absolute value $|f|$ and the phase δ_D as $f_{D^0}(m^2_+, m^2_-) = |f|e^{i\delta_D}$. The $\bar{D}^0$ amplitude is written as $f_{\bar{D}^0}(m^2_+, m^2_-) = f_{D^0}(m^2_-, m^2_+)$ ignoring the small second-order charm mixing [7] and direct CP violation effects [6]. The amplitude of the $B^- \to D^0K^-$ decay is rewritten as

$$\begin{aligned} f_B(m^2_+, m^2_-) &\propto |f_{D^0}(m^2_+, m^2_-)|e^{i\delta_D(m^2_+, m^2_-)} + r_B e^{i(\delta_B-\gamma)}|f_{D^0}(m^2_-, m^2_+)|e^{i\delta_D(m^2_-, m^2_+)} \\ &\propto |f_{D^0}(m^2_+, m^2_-)| + r_B e^{i(\delta_B-\gamma)}|f_{D^0}(m^2_-, m^2_+)|e^{i(\delta_D(m^2_+, m^2_-)-\delta_D(m^2_-, m^2_+))}. \end{aligned} \tag{1.2}$$

Therefore, determination of the γ angle requires input of the strong-phase difference between D^0 and $\bar{D}^0 \to K^0_S\pi^+\pi^-$ decays, i.e., $\Delta\delta_D = \delta_D(m^2_+, m^2_-) - \delta_D(m^2_-, m^2_+)$. In addition, due to the abundant intermediate processes in the $D \to K^0_S\pi^+\pi^-$ decay, $\Delta\delta_D$ varies in phase space, making this channel the most sensitive to the γ angle.

The strong-phase difference $\Delta\delta_D$ between D^0 and $\bar{D}^0 \to K^0_S\pi^+\pi^-$ decays can be modeled using an amplitude analysis based on the experimental data of $D^0 \to K^0_S\pi^+\pi^-$. However, this approach introduces unavoidable model dependence, complicating the estimation of the systematic uncertainty associated with different model choices in the γ measurement [8]. Alternatively, quantum-correlated (QC) $D\bar{D}$ pairs produced at the $\psi(3770)$ resonance provides an ideal environment to determine $\Delta\delta_D$ [6]. This method allows for a model-independent measurement of the γ angle [9], where the uncertainty from the strong-phase difference can be reliably estimated.

Furthermore, the strong-phase difference $\Delta\delta_D$ between D^0 and $\bar{D}^0 \to K^0_S\pi^+\pi^-$ decays can provide inputs to determine another UT angle β [10], for the study of charm mixing and CP violation phenomena [11]. Additionally, it aids in the measurement of the strong-phase differences in various other D^0 hadronic decays [12].

The CLEO experiment determined the strong-phase difference between D^0 and $\bar{D}^0 \to K^0_S\pi^+\pi^-$ decays for the first time, using a dataset collected at the $\psi(3770)$ resonance with an integrated luminosity of $0.818\,\text{fb}^{-1}$ [13]. The BESIII experiment subsequently measured these parameters using a larger $\psi(3770)$ dataset of $2.93\,\text{fb}^{-1}$ [14]. Recently, BESIII has further expanded its data collection, and the total integrated luminosity of the $\psi(3770)$ data sample is $7.93\,\text{fb}^{-1}$ [15]. This enables a more precise determination of the strong-phase differences, thereby reducing the associated uncertainty in determining the angle γ.

The strong-phase difference parameters in the $D^0 \to K^0_L\pi^+\pi^-$ decay were also measured in the previous analysis to improve the determination of those in the $D^0 \to K^0_S\pi^+\pi^-$ decay [13, 14]. A model-dependent constraint, derived from the differences between the strong-phase parameters in $D^0 \to K^0_S\pi^+\pi^-$ and $D^0 \to K^0_L\pi^+\pi^-$ decays, was employed to improve the precision. Recently, the BESIII experiment has implemented the amplitude

JHEP06(2025)086

analysis of the $D^0 \to K^0_L\pi^+\pi^-$ decay [16], and the resultant model provides an improved estimation of the model-constraint in this analysis. Moreover, with the larger $\psi(3770)$ data sample at BESIII, it is now feasible to remove the model-dependent constraint entirely. This development allows for a detailed study of its impact on the measurement of the strong-phase parameters and the angle γ, and for improved knowledge of the strong-phase differences in both $D^0 \to K^0_S\pi^+\pi^-$ and $D^0 \to K^0_L\pi^+\pi^-$ decays.

In this paper, we present an improved measurement of the strong-phase parameters in $D \to K^0_{S,L}\pi^+\pi^-$ decays using the BESIII $\psi(3770)$ dataset with an integrated luminosity of $7.93\,\text{fb}^{-1}$. The paper is organized as follows: in section 2, the definition and theoretical formalism of strong-phase difference parameters are discussed. Section 3 provides an introduction to the BESIII detector, the data samples and the simulated Monte Carlo (MC) samples. The most recent amplitude models are implemented in these MC samples, resulting in an improved simulation of the QC effects, thereby reducing the associated systematic uncertainties in this study. The event criteria, background estimation and fitted yields are detailed in section 4. The model-independent results of the strong-phase difference parameters and the related systematic uncertainties are presented in section 5. Finally, the impact of the strong-phase parameters on the γ measurement is assessed in section 6.

2 Formalism

This analysis utilizes $D \to K^0_S\pi^+\pi^-$ phase space, which is divided into bins according to three schemes identical to those used in ref. [13]. These bins in the Dalitz plot are symmetric with respect to the $m^2_+ = m^2_-$ axis and are indexed by i from -8 to 8, excluding zero. Positive (negative) bins are located in the $m^2_+ > m^2_-$ ($m^2_+ < m^2_-$) region.[1] The binning schemes are illustrated in figure 1, denoted as the equal binning scheme, the optimal binning scheme and the modified optimal binning scheme. The detailed information on the choice of these regions is given in ref. [13].

The strong-phase difference $\Delta\delta_D$, which quantifies the interference between the amplitudes of D^0 and $\bar{D}^0$ decays, is parameterized using the amplitude-weighted averages of $\cos\Delta\delta_D$ and $\sin\Delta\delta_D$ in each bin. These parameters are defined as

$$\begin{aligned} c_i &= \frac{1}{\sqrt{F_i F_{-i}}} \int_i |f_{D^0}(m^2_+, m^2_-)||f_{D^0}(m^2_-, m^2_+)| \cos[\Delta\delta_D(m^2_+, m^2_-)]\mathrm{d}m^2_+\mathrm{d}m^2_-, \\ s_i &= \frac{1}{\sqrt{F_i F_{-i}}} \int_i |f_{D^0}(m^2_+, m^2_-)||f_{D^0}(m^2_-, m^2_+)| \sin[\Delta\delta_D(m^2_+, m^2_-)]\mathrm{d}m^2_+\mathrm{d}m^2_-, \end{aligned} \tag{2.1}$$

where F_i represents the fraction of events found in the i^{th} bin of the flavour-specific decay $D^0 \to K^0_S\pi^+\pi^-$.

Using the large dataset collected at the $\psi(3770)$ resonance, where neutral $D\bar{D}$ decays exhibit C-odd correlations, the strong-phase parameters are accessed by tagging both D mesons [6]. This approach is denoted as the double-tag (DT) method. The tag modes reconstructed against the signal $K^0_{S/L}\pi^+\pi^-$ decays fall into the categories of flavour, CP eigenstate or self-conjugate, as detailed in table 1.

[1] There was a typo in the definition of the bin numbering in the previous publication [14].

JHEP06(2025)086

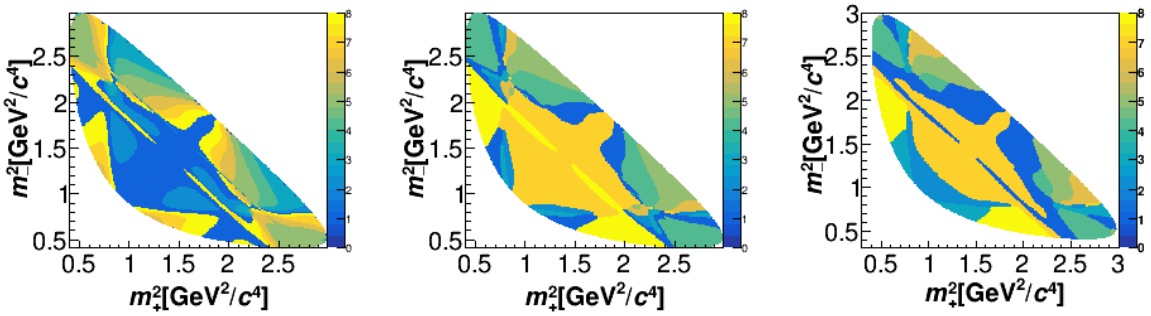

Figure 1. Binned regions marked as different colors indexed from 1 to 8 in the equal binning scheme (left), optimal binning scheme (middle) and modified-optimal binning scheme (right).

Flavour	$K^+e^-\nu_e$, $K^+\pi^-\pi^+\pi^-$, $K^+\pi^-\pi^0$, $K^+\pi^-$
CP-even	K^+K^-, $\pi^+\pi^-$, $\pi^+\pi^-\pi^0$, $K^0_S\pi^0\pi^0$, $K^0_L\pi^0$
CP-odd	$K^0_S\pi^0$, $K^0_S\eta_{\gamma\gamma}$, $K^0_S\eta_{\pi^+\pi^-\pi^0}$, $K^0_S\omega$, $K^0_S\eta'_{\gamma\rho}$, $K^0_S\eta'_{\pi\pi\eta}$, $K^0_L\pi^0\pi^0$
Self-conjugate	$K^0_S\pi^+\pi^-$, $K^0_S(\pi)_{\rm miss}\pi$, $(\pi^0(\pi^0)_{\rm miss})_{K^0_S}\pi\pi$

Table 1. Tag modes reconstructed against the signal decays. The partially-reconstructed tag modes of $K^+e^-\nu_e$, $K^0_L\pi^0$, $K^0_L\pi^0\pi^0$, $K^0_S(\pi)_{\rm miss}\pi$ and $(\pi^0(\pi^0)_{\rm miss})_{K^0_S}\pi\pi$ tags are not used for the $K^0_L\pi^+\pi^-$ decay.

For DT events in which one D meson decays into the signal mode $K^0_S\pi^+\pi^-$ and the other into a *CP* eigenstate, the decay amplitude is expressed as

$$f_{CP\pm}(m^2_+, m^2_-) = \frac{1}{\sqrt{2}}(f_D(m^2_+, m^2_-) \pm f_D(m^2_-, m^2_+)), \tag{2.2}$$

where $\pm$ denotes the *CP* eigenvalue of different tag modes. The expected number of signal events in the $i^{\rm th}$ bin, denoted as M_i for the signal mode $K^0_S\pi^+\pi^-$, is derived by integrating the square of the amplitude over the bin

$$M_i \propto K_i + K_{-i} - (2F^+_{CP} - 1) \times 2c_i\sqrt{K_iK_{-i}}, \tag{2.3}$$

where $K_i \propto \int_i |f_{D^0}(m^2_+, m^2_-)|^2 dm^2_+ dm^2_-$ represents the flavour-specific $K^0_S\pi^+\pi^-$ decay events in the $i^{\rm th}$ bins. F^+_{CP} denotes the *CP*-even fraction of the tag mode, taking a value of 1 (0) for *CP*-even (odd) eigenstate.

To further constrain the strong-phase parameters, the signal mode $K^0_S\pi^+\pi^-$ is tagged with self-conjugate tags, i.e. $K^0_S\pi^+\pi^-$ versus $K^0_S\pi^+\pi^-$. In this context, the decay amplitude is written as

$$f = \frac{1}{\sqrt{2}}\left[f_D(m^2_+, m^2_-)f_D(m^{2\dagger}_-, m^{2\dagger}_+) - f_D(m^{2\dagger}_+, m^{2\dagger}_-)f_D(m^2_-, m^2_+)\right], \tag{2.4}$$

where the symbol † differentiates the Dalitz plot coordinates between the two $K^0_S\pi^+\pi^-$ decays. The event rate M_{ij}, defined as the event yields observed in the $i^{\rm th}$ bin of the first and $j^{\rm th}$ bin of the second $D \to K^0_S\pi^+\pi^-$ Dalitz plot, is expressed as

$$M_{ij} \propto K_iK_{-j} + K_{-i}K_j - 2\sqrt{K_iK_{-i}K_jK_{-j}}(c_ic_j + s_is_j). \tag{2.5}$$

JHEP06(2025)086

In this analysis, the $K^0_S\pi^+\pi^-$ tag is reconstructed using three independent selection methods to improve precision. These methods are denoted as the fully reconstructed $K^0_S\pi^+\pi^-$ tag, the missing π tag $K^0_S(\pi)_{\rm miss}\pi$ and the missing π^0 tag $(\pi^0(\pi^0)_{\rm miss})_{K^0_S}\pi\pi$.

Taking advantage of the *CP* relationship between $D \to K^0_L\pi^+\pi^-$ and $D \to K^0_S\pi^+\pi^-$ decays, it is helpful to include $D \to K^0_L\pi^+\pi^-$ as a self-conjugate tag mode to further enhance the precision of the measurement. The event rate of $K^0_S\pi^+\pi^-$ versus $K^0_L\pi^+\pi^-$ DT sample, denoted as M'_{ij}, is given by

$$M'_{ij} \propto K_i K'_{-j} + K_{-i} K'_j + 2\sqrt{K_i K_{-i} K'_j K'_{-j}}(c_i c'_j + s_i s'_j). \tag{2.6}$$

Here, c'_i and s'_i represent the strong-phase parameters associated with the $D \to K^0_L\pi^+\pi^-$ decay, and K'_i denotes the yield of flavour-specific $K^0_L\pi^+\pi^-$ DT decays. They are defined analogously to those for the $D \to K^0_S\pi^+\pi^-$ decay, following the binning schemes shown in figure 1.

To better constrain the strong-phase difference parameters in the $D \to K^0_L\pi^+\pi^-$ decay, the DT events of $K^0_L\pi^+\pi^-$ versus *CP* eigenstates are selected. The decay rate M'_i is expressed as

$$M'_i \propto K'_i + K'_{-i} + (2F^+_{CP} - 1) \times 2c'_i\sqrt{K'_i K'_{-i}}. \tag{2.7}$$

The expected DT yields in eqs. (2.3) and (2.5), (2.6) and (2.7) are normalized using the single-tag (ST) yields. ST events are defined for the events that have only one of the two D-meson decays detected. By normalizing DT signal yields with the ST yields, the associated systematic uncertainties are significantly reduced. For the tag modes that are partially reconstructed in table 1, the ST yields are calculated based on the knowledge of the branching fractions of the tag modes [17].

3 BESIII detector

The BESIII detector [18] records symmetric e^+e^- collisions provided by the BEPCII storage ring [19] in the center-of-mass energy range from 1.84 to 4.95 GeV with a peak luminosity of $1.1 \times 10^{33}\,\mathrm{cm^{-2}\,s^{-1}}$ achieved at $\sqrt{s} = 3.773\,\mathrm{GeV}$. BESIII has collected large data samples in this energy region [20–22]. The cylindrical core of the BESIII detector covers 93% of the full solid angle and consists of a helium-based multilayer drift chamber (MDC), a plastic scintillator time-of-flight system (TOF), and a CsI(Tl) electromagnetic calorimeter (EMC), which are all enclosed in a superconducting solenoidal magnet providing a 1.0 T magnetic field, which was 0.9 T in 2012. The solenoid is supported by an octagonal flux-return yoke with resistive plate counter muon identification modules interleaved with steel.

The charged-particle momentum resolution at 1 GeV/c is 0.5%, and the dE/dx resolution is 6% for electrons from Bhabha scattering. The EMC measures photon energies with a resolution of 2.5% (5%) at 1 GeV in the barrel (end cap) region. The time resolution in the TOF barrel region is 68 ps, while that in the end cap region was 110 ps. The end cap TOF system was upgraded in 2015 using multigap resistive plate chamber technology, providing a time resolution of 60 ps [23]. This update benefits 63% of the data used in this analysis. More details can be checked in ref. [18].

Monte Carlo (MC) simulated data samples produced with GEANT4-based [24] software, which includes the geometric description of the BESIII detector and the detector response,

JHEP06(2025)086

are used to determine detection efficiencies and to estimate backgrounds. The simulation models the beam energy spread and initial state radiation (ISR) in the e^+e^- annihilations with the generator KKMC [25, 26].

Inclusive MC samples are produced including the $D\bar{D}$ pairs corrected for the QC effects, the non-$D\bar{D}$ decays of the $\psi(3770)$, the ISR production of the J/ψ and $\psi(3686)$ states, and the continuum processes incorporated in KKMC [25, 26]. All particle decays in the inclusive MC sample are modeled with EVTGEN [27, 28] using branching fractions either taken from the Particle Data Group [17], when available, or otherwise estimated with LUNDCHARM [29, 30]. In particular, the $D^0 \to \pi^+\pi^-\pi^+\pi^-$ and $D^0 \to \pi^+\pi^-\pi^0\pi^0$ decays, which are the major peaking backgrounds in the $K^0_S\pi^+\pi^-$ signal decay, are modified in the inclusive MC samples according to their amplitude models [31]. Final state radiation from charged final state particles is incorporated using PHOTOS [32].

The signal MC samples are simulated for the DT $K^0_{S/L}\pi^+\pi^-$ versus tag modes, where the QC effects are implemented. The $K^0_S\pi^+\pi^-$ decay is simulated with the amplitude model measured by the Belle experiment [33]. The $K^0_L\pi^+\pi^-$ decay is simulated with the $K^0_S\pi^+\pi^-$ model implemented with the U-spin breaking parameters [16]. Multibody tag-side decays are simulated with EVTGEN [27, 28] according to the most recent models from experimental studies.

4 Event selection and signal yield

4.1 Event selection

Final-state particles in ST and DT decays are reconstructed from candidates of charged tracks and photons. The selection criteria for charged tracks and photons and intermediate resonances such as π^0, K^0_S, η, η' and ω are identical to those described in ref. [14]. Specifically, the invariant mass $M_{\pi^+\pi^-}$ for the K^0_S candidates is optimized to be within $(0.487, 0.511)\,\mathrm{GeV}/c^2$ and the invariant mass $M_{\gamma\pi^+\pi^-}$ for the η' candidates must be within $(0.940, 0.970)\,\mathrm{GeV}/c^2$.

Decays of D mesons are reconstructed into either tag modes as detailed in table 1 or the $K^0_{S/L}\pi^+\pi^-$ signal mode. When all final state particles are reconstructed, the tags are denoted as fully reconstructed tags. To suppress combinatorial background in the fully reconstructed tags, a mode-specific requirement on the energy difference between the beam and the final states $\Delta E = E_{D^0} - \sqrt{s}/2$ is applied [14], where $\sqrt{s}/2$ represents the energy of the electron beam, and E_{D^0} is the reconstructed energy of the D candidate. If multiple candidates are selected in an event, the one with the smallest $|\Delta E|$ is chosen as the best candidate. The beam-constrained mass, $M_{\mathrm{BC}} = \sqrt{(\sqrt{s}/2)^2 - |\boldsymbol{p}_{D^0}|^2}$, is utilized as the variable to determine both ST and DT yields, where $\boldsymbol{p}_{D^0}$ represents the reconstructed momentum of the D candidate.

When a missing particle, such as the K^0_L meson, is present in the final states, the tags are partially reconstructed. In such cases, the "missing mass" method described in ref. [14] is utilized. The squared missing mass M^2_{miss} is defined as $M^2_{\mathrm{miss}} = E^2_{\mathrm{miss}} - |\boldsymbol{p}_{\mathrm{miss}}|^2$, where $E_{\mathrm{miss}} = \sqrt{s}/2 - E_{\mathrm{other}}$, $\boldsymbol{p}_{\mathrm{miss}} = -\boldsymbol{p}_{\mathrm{tag}} - \boldsymbol{p}_{\mathrm{other}}$. Here, $\boldsymbol{p}_{\mathrm{tag}}$ represents the momentum of the fully reconstructed signal $D \to K^0_S\pi^+\pi^-$ decay, while $\boldsymbol{p}_{\mathrm{other}}$ and E_{other} are the momentum and energy of the other reconstructed particles that form the partially-reconstructed tags. Correctly reconstructed events are expected to peak at the squared mass of the missing particle in the M^2_{miss} distribution. Therefore the M^2_{miss} variable is used to determine the

JHEP06(2025)086

DT yield. In the selection of the $K^+e^-\nu_e$ mode, the variable $U_{\rm miss} = E_{\rm miss} - |\boldsymbol{p}_{\rm miss}|$ is employed as the fit variable. Correctly reconstructed events with a missing neutrino are expected to peak around $U_{\rm miss} = 0$.

For DT candidates where $K^0_S\pi^+\pi^-$ signal events are tagged by fully reconstructed modes, the selection is based on the ΔE and $M_{\rm BC}$ variables for both signal and tag sides. The selection criteria of ΔE are identical to those applied to ST candidates.

For partially-reconstructed DT candidates whose final states contain a K^0_L meson, it is required that there are no extra charged tracks or $\gamma\gamma$ candidates for π^0 or η particles. For the $K^0_S\pi^+\pi^-$ signal tagged by the partially-reconstructed $K^0_S\pi^+\pi^-$ mode, DT events containing extra charged tracks are rejected. For the signal $K^0_S\pi^+\pi^-$ events tagged with the $K^0_L\pi^0\pi^0$ decay, the recoil mass of either π^0 is required to be larger than $0.7\,{\rm GeV}/c^2$ to suppress the background of $D^0 \to \pi^0\pi^0\pi^0$ decay. Furthermore, the mass of any $K^0_S\pi^\pm\pi^0$ combination is required to be out of the D^+ mass region $(1.85, 1.89)\,{\rm GeV}/c^2$ to suppress the $D^+ \to K^0_{S/L}\pi^+\pi^0$ versus $D^- \to K^0_{L/S}\pi^-\pi^0$ backgrounds. The DT $K^0_L\pi^+\pi^-$ versus $K^0_S\pi^0\pi^0$ events are also subjected to the above requirement.

To mitigate resolution effects in DT samples, kinematic fits are performed to constrain the D mass, K^0_S mass and K^0_L mass. If there are multiple candidates in a DT event, the best candidate is selected following the methodology used in ref. [14].

4.2 Background study

The inclusive MC samples are utilized to investigate the possible sources of peaking background. For the ST flavour mode $K^+\pi^-\pi^+\pi^-$, the dominant peaking background originates from the $K^0_SK^\pm\pi^\mp$ decay, with the background fractions of approximately 2.4%. In the *CP*-eigenstate channels, $\pi^+\pi^-\pi^0\pi^0$, $\pi^+\pi^-\pi^0$ and $K^0_S\pi^0$ are the major peaking backgrounds in the $K^0_S\pi^0\pi^0$, $K^0_S\pi^0$ and $\pi^+\pi^-\pi^0$ tags, with the background fractions of around 4.2%, 0.5% and 6.7%, respectively. In the $K^0_S\eta_{\pi^+\pi^-\pi^0}$ and $K^0_S\omega$ tag modes, non-resonant $K_S\pi^+\pi^-\pi^0$ decay is identified as the dominant peaking background. The corresponding exclusive MC samples are simulated to obtain the contamination rates, which are found to be about 8% and 12% in the $K^0_S\eta_{\pi^+\pi^-\pi^0}$ and $K^0_S\omega$ tags, respectively.

In DT $K^0_S\pi^+\pi^-$ decays, the major peaking backgrounds on the signal side arise from the $\pi^+\pi^-\pi^+\pi^-$ and $K^0_SK^0_S$ decays, with the background fractions of around 0.25% and 0.4%, respectively. The tag side of fully reconstructed modes exhibits the same sources of peaking background as observed in ST events. In partially reconstructed tag modes where the tag side is $K^0_LX(X = \pi^0, \pi^0\pi^0)$ decays, the major peaking background comes from K^0_SX, primarily through the decay $K^0_S \to \pi^0\pi^0$, with the background fractions of approximately 8% and 16%, respectively. Furthermore, the dominant background becomes $\pi^+\pi^-\pi^+\pi^-$ for $K^0_S(\pi)_{\rm miss}\pi$ and $\pi^+\pi^-\pi^0\pi^0$ for $(\pi^0(\pi^0)_{\rm miss})_{K^0_S}\pi\pi$ tag modes, with the background fractions of approximately 3% and 13%, respectively.

In DT $K^0_L\pi^+\pi^-$ decays, the $K^0_S\pi^+\pi^-$ decay is identified as the principal source of peaking background on the signal side, with a contamination rate of approximately 10%. To minimize the systematic uncertainties, the background contribution is assessed using the signal yields determined in this analysis. Additionally, $\pi^+\pi^-\eta$ constitutes a notable peaking background, with a fraction of 1%. Since the $D \to K^0_L\pi^+\pi^-$ decays are tagged by

JHEP06(2025)086

Mode	$N_{\rm ST}$	$\epsilon_{\rm ST}$	$N_{\rm DT}^{K^0_S\pi^+\pi^-}$	$\epsilon_{\rm DT}^{K^0_S\pi^+\pi^-}$	$N_{\rm DT}^{K^0_L\pi^+\pi^-}$	$\epsilon_{\rm DT}^{K^0_L\pi^+\pi^-}$
$K^+\pi^-$	1449322 ± 1262	65.3 ± 0.0	12159 ± 122	26.1 ± 0.1	27492 ± 180	40.5 ± 0.1
$K^+\pi^-\pi^0$	2913155 ± 2011	35.6 ± 0.0	23337 ± 172	13.6 ± 0.1	53536 ± 257	21.6 ± 0.1
$K^+\pi^-\pi^+\pi^-$	1944170 ± 1571	40.8 ± 0.0	15341 ± 143	16.0 ± 0.1	33178 ± 205	21.8 ± 0.1
$K^+e^-\nu_e$	—	—	8835 ± 107	21.1 ± 0.1	—	—
$\pi^+\pi^-\pi^0$	300905 ± 1131	37.1 ± 0.1	2280 ± 53	15.3 ± 0.0	7540 ± 127	25.2 ± 0.0
$\pi^+\pi^-$	55461 ± 296	64.5 ± 0.1	431 ± 21	25.1 ± 0.1	1322 ± 43	41.3 ± 0.1
K^+K^-	150181 ± 421	61.0 ± 0.1	1124 ± 37	24.3 ± 0.1	3783 ± 66	38.7 ± 0.1
$K^0_S\pi^0\pi^0$	65631 ± 409	16.6 ± 0.2	392 ± 24	6.2 ± 0.0	1325 ± 47	9.2 ± 0.0
$K^0_L\pi^0$	—	—	1969 ± 48	17.9 ± 0.1	—	—
$K^0_S\pi^0$	190361 ± 471	40.3 ± 0.3	1640 ± 43	14.8 ± 0.0	2547 ± 66	22.6 ± 0.1
$K^0_S\eta_{\gamma\gamma}$	26016 ± 195	33.4 ± 0.2	221 ± 15	12.0 ± 0.1	313 ± 25	19.2 ± 0.1
$K^0_S\eta'_{\pi\pi\eta}$	9262 ± 105	14.5 ± 0.0	67 ± 9	5.2 ± 0.1	126 ± 13	8.2 ± 0.1
$K^0_S\eta_{\pi\pi\pi^0}$	9006 ± 119	19.6 ± 0.1	57 ± 8	6.5 ± 0.1	121 ± 15	10.5 ± 0.1
$K^0_S\eta'_{\pi\pi\gamma}$	23015 ± 195	19.9 ± 0.1	175 ± 14	7.2 ± 0.1	320 ± 22	11.4 ± 0.1
$K^0_S\omega$	72787 ± 375	17.3 ± 0.1	564 ± 27	6.0 ± 0.0	967 ± 44	9.8 ± 0.1
$K^0_L\pi^0\pi^0$	—	—	908 ± 33	6.6 ± 0.0	—	—
$K^0_S\pi^+\pi^-$	—	—	2302 ± 57	18.5 ± 0.0	8506 ± 103	22.0 ± 0.0
$K^0_S(\pi)_{\rm miss}\pi$	—	—	572 ± 28	4.4 ± 0.0	—	—
$(\pi^0(\pi^0)_{\rm miss})_{K^0_S\pi\pi}$	—	—	1715 ± 49	16.6 ± 0.0	—	—

Table 2. Results of the ST yields ($N_{\rm ST}$), ST efficiency ($\epsilon_{\rm ST}$), DT yields ($N_{\rm DT}^{K^0_S\pi^+\pi^-}$) for $K^0_S\pi^+\pi^-$ signals and the corresponding DT efficiency ($\epsilon_{\rm DT}^{K^0_S\pi^+\pi^-}$), as well as DT yields ($N_{\rm DT}^{K^0_L\pi^+\pi^-}$) for $K^0_L\pi^+\pi^-$ signals and the corresponding DT efficiency ($\epsilon_{\rm DT}^{K^0_L\pi^+\pi^-}$), where the uncertainties are statistical. The efficiencies are in units of percentage.

fully reconstructed modes, the peaking backgrounds on the tag side are the same as those in the corresponding selected ST events.

4.3 Signal yields and efficiencies

The ST yields of the fully reconstructed tag modes are obtained through unbinned maximum likelihood fits on the $M_{\rm BC}$ distributions. The signal shape is obtained from the signal MC samples, but is convolved with Gaussian functions to accommodate the resolution differences between data and MC simulations. The mean values and widths of the Gaussian functions are free parameters of the fits. Peaking backgrounds are subtracted according to the inclusive MC samples. An ARGUS function [34], with its endpoint fixed at the beam energy and other parameters determined from the fit, models the combinatorial backgrounds. The outcomes of these fits are depicted in figure 2, and the resulting signal yields are tabulated in table 2.

The DT yields are determined both within every bin of the phase space and across the entire phase space. For each fully reconstructed mode, signal yields are obtained through

JHEP06(2025)086

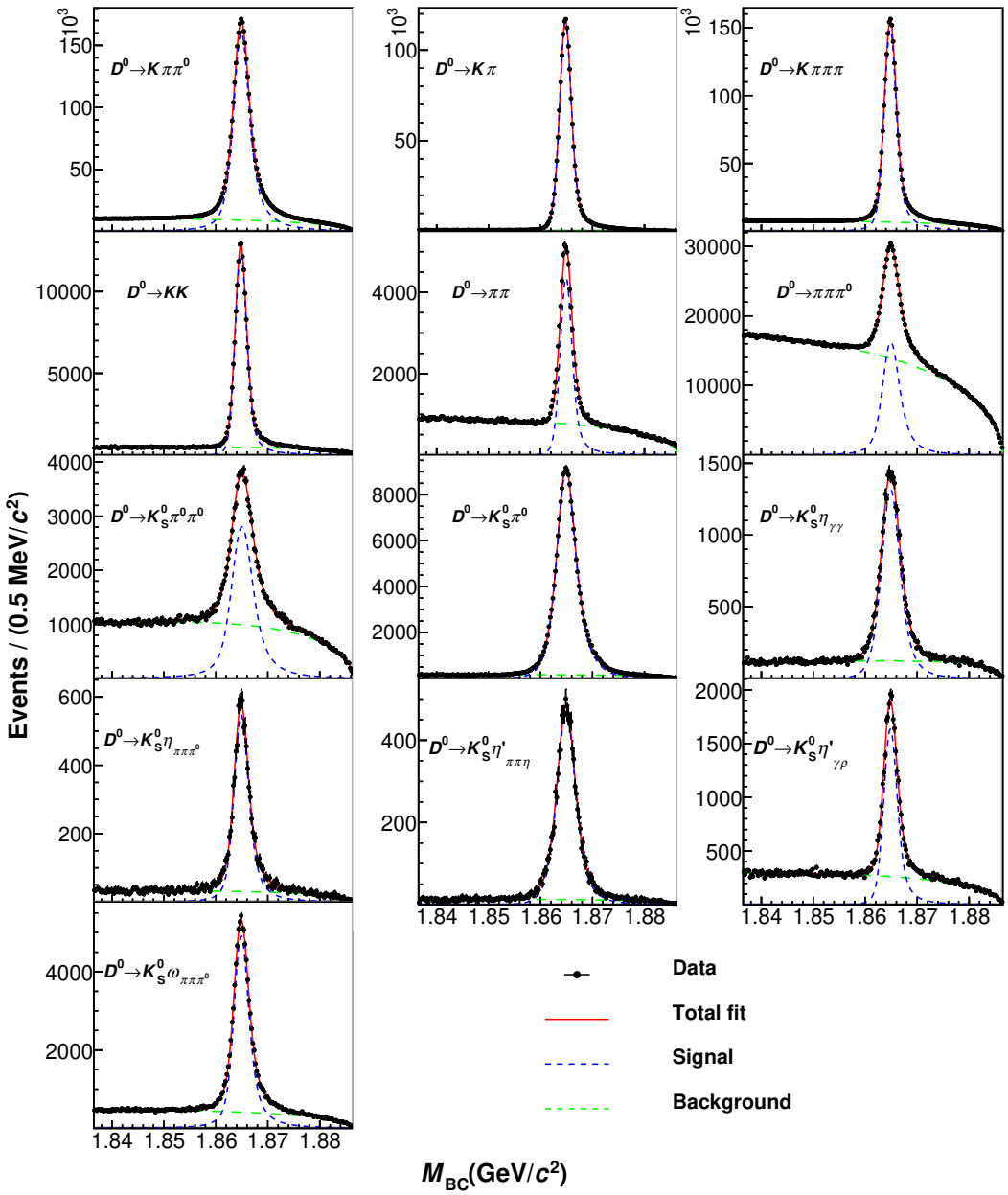

Figure 2. Fits to the $M_{\rm BC}$ distributions of ST signal events. The black points with error bars represent data where peaking background has been subtracted. The red solid lines represent the fit to data. The signal and background components are shown as blue and green dashed lines.

one-dimensional (1D) unbinned maximum likelihood fits of the signal-side $M_{\rm BC}$ distributions. The fits across entire phase space are shown in figure 3 for all fully reconstructed DT events and the logarithmic-scale fits are shown in figure 9. The signal shapes are derived from signal MC samples and convolved with Gaussian functions. Peaking background and the background from D^+D^- decays are fixed according to the inclusive MC simulations. Other continuum backgrounds, dominated by the $e^+e^-\to q\bar{q}$ process, are modeled using the MC-simulated shape with their contribution left free in the fits.

JHEP06(2025)086

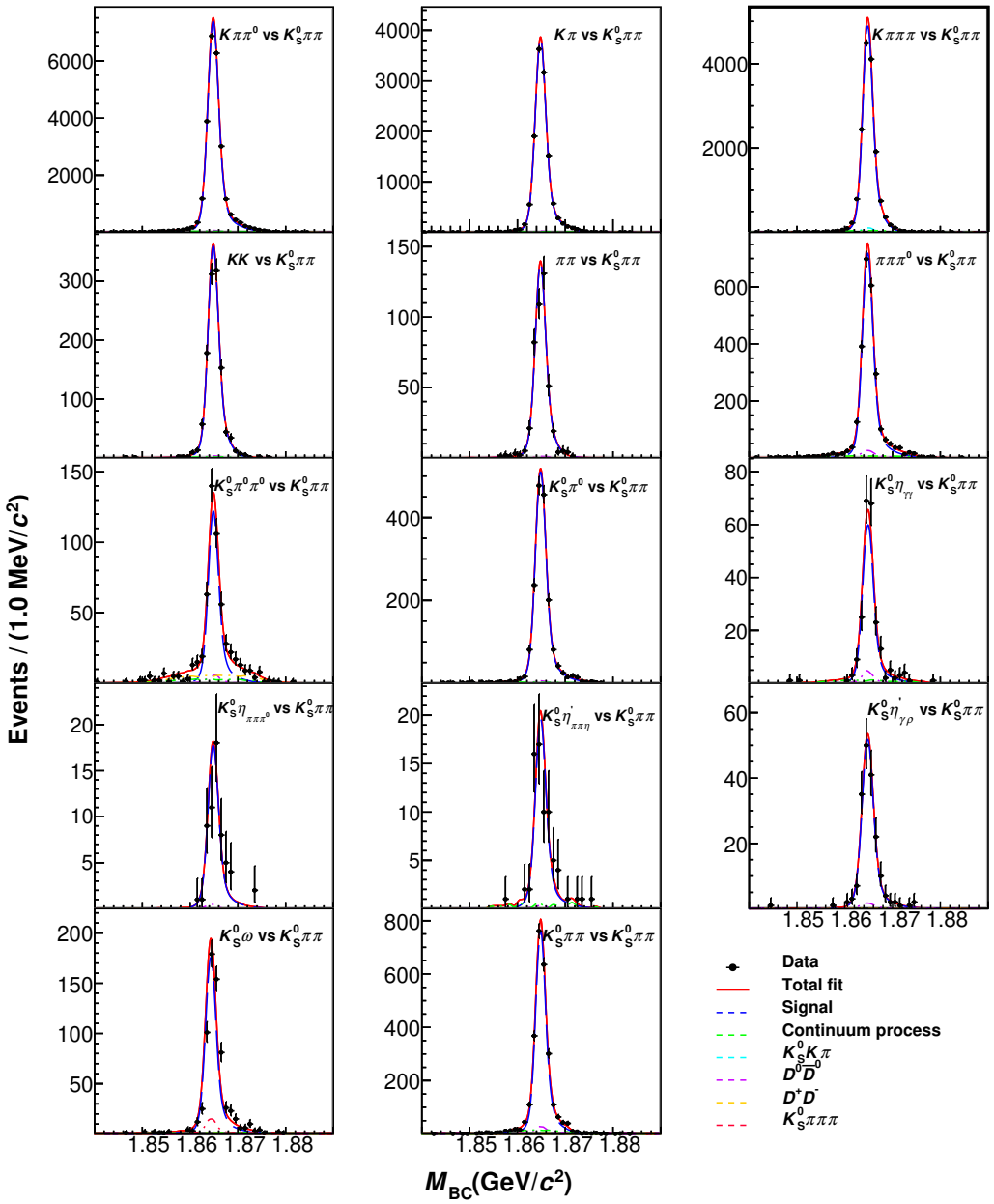

Figure 3. The 1D unbinned maximum likelihood fits for $K^0_S\pi^+\pi^-$ versus full reconstructed modes on $M_{\rm BC}$. The black points with error bars represent data. The dashed lines indicate the signal and background shapes. The red lines represent the sum of signal and background shapes. The fitting plots in logarithm scale are shown in figure 9.

In the partially reconstructed modes, such as $K^0_L X$, missing π and missing π^0, 1D unbinned maximum likelihood fits are performed to the $M^2_{\rm miss}$ distributions. For the $K^+e^-\nu_e$ tag mode, the fit is applied to the $U_{\rm miss}$ distribution. These fit results are shown in figure 4 and the logarithmic-scale fits are shown in figure 10. The determination of the signal component, peaking background, D^+D^- background and continuum processes follow the same methodology as used for fully reconstructed tags. Notably, in signal events tagged by the $K^0_L\pi^0\pi^0$ mode or the $(\pi^0(\pi^0)_{\rm miss})_{K^0_S}\pi\pi$ mode, photons might swap between the two

JHEP06(2025)086

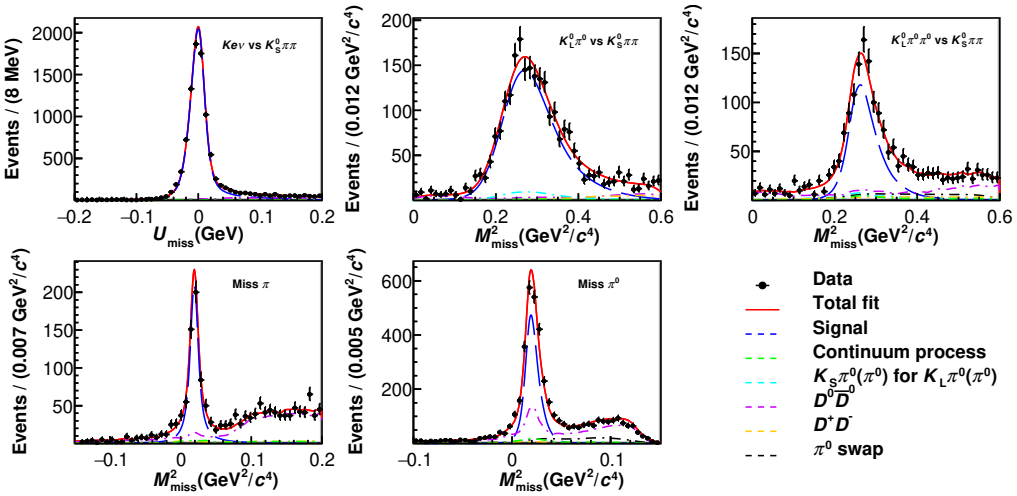

Figure 4. The 1D unbinned maximum likelihood fits for $K^0_S\pi^+\pi^-$ versus partially reconstructed tags on $M^2_{\rm miss}/U_{\rm miss}$. The black points with error bars represent data. The dashed lines indicate the signal and background shapes. The red lines represent the sum of signal and background shapes. The fitting plots in logarithm scale are shown in figure 10.

π^0's in the tag side, which introduces a flat combinatorial background. The ratio of this background to the signal yield is fixed according to signal MC simulations.

The fits to the $M^2_{\rm miss}$ distributions for $K^0_L\pi^+\pi^-$ decays tagged with fully reconstructed tag modes are shown in figure 5. The fit results in logarithm scale are plotted in figure 11. Peaking background is fixed according to the inclusive MC simulations. Combinatorial backgrounds in these fits arise from D^+D^- decays, $D^0\bar{D}^0$ decays and continuum processes. The shapes of both signal and combinatorial background components are derived from the MC samples. For the DT $K^0_L\pi^+\pi^-$ versus $\pi^+\pi^-\pi^0$ case, the background contribution from the process $e^+e^-\to\tau^+\tau^-$, which is non-negligible, is fixed according to the inclusive MC samples.

The ST and DT efficiencies are determined through simulated MC samples. For the tracking and PID efficiencies of pions and K^0_S reconstruction efficiency, their differences between data and MC simulations are studied with a control sample of hadronic $D\bar{D}$ events. These differences are corrected for in the detection efficiency of the decay modes of $K^0_S\pi^+\pi^-$, $K^0_S(\pi)_{\rm miss}\pi$, $(\pi^0(\pi^0)_{\rm miss})_{K^0_S}\pi\pi$, and $K^0_L\pi^+\pi^-$. However, the efficiency corrections are not applied to the fully reconstructed tag modes, as their detection efficiencies largely cancel out in the ratio of the ST and DT yields. Furthermore, the difference of reconstruction efficiency is found to be negligible for the $K^+e^-\nu_e$ tag. The resultant efficiencies are listed in table 2.

5 Measurement of $c_i^{(\prime)}$ and $s_i^{(\prime)}$ parameters

5.1 Determination of the $K_i^{(\prime)}$ parameters

The efficiency-corrected binned yields of flavour-specific $D^0\to K^0_{S/L}\pi^+\pi^-$ decays, denoted as $K_i^{(\prime)}$, are necessary to determine the expected yields in the decays sensitive to the strong-phase difference parameters. $K_i^{(\prime)}$ is calculated from the observed yields $N_i^{{\rm obs}(\prime)}$ in the $i^{\rm th}$ bin of flavour tags via $K_i^{(\prime)}=\sum_{j=-8}^{8}[(\epsilon^{(\prime)})^{-1}]_{ij}N_j^{{\rm obs}(\prime)}$, where the efficiency matrix $\epsilon_{ij}^{(\prime)}$ denotes the

JHEP06(2025)086

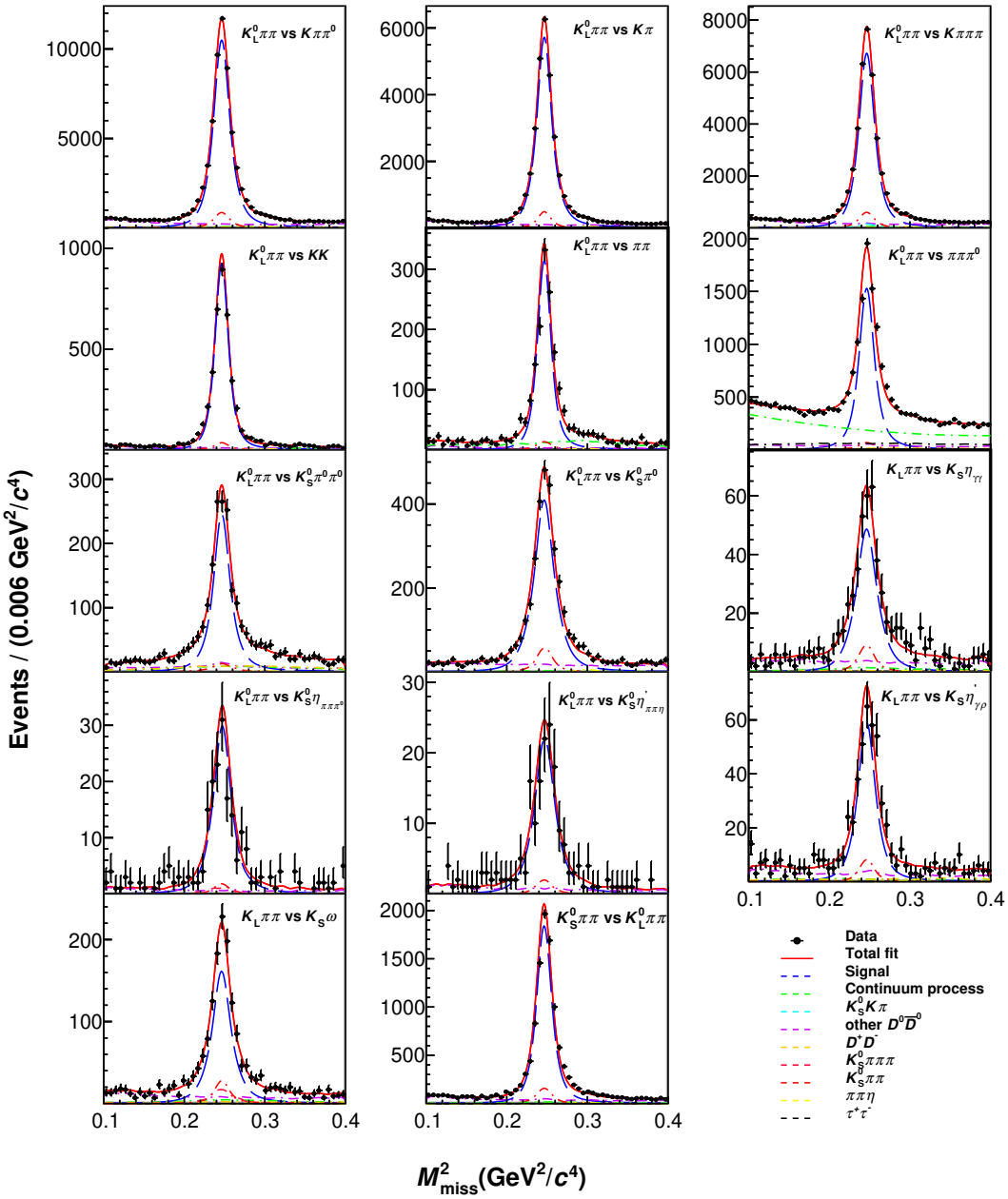

Figure 5. The 1D unbinned maximum likelihood fits for $K^0_L\pi^+\pi^-$ versus various tag modes on $M^2_{\rm miss}$. The black points with error bars represent data. The dashed lines indicate the signal and background shapes. The red lines represent the sum of signal and background shapes. The fitting plots in logarithm scale are shown in figure 11.

efficiency correction matrix determined with MC simulations. This matrix describes the experimental migration effect when a signal event is produced in the $j^{\rm th}$ bin but reconstructed in the $i^{\rm th}$ bin.

Doubly Cabibbo-suppressed (DCS) processes include the hadronic flavoured tags $K^+\pi^-$, $K^+\pi^-\pi^0$ and $K^+\pi^-\pi^+\pi^-$. The DCS contribution must be subtracted because they lead to incorrect assignments of the charm quantum number. To account for this effect, the $K^0_{S/L}\pi^+\pi^-$ signal events are scaled by correction factors. These factors are calculated according to eq. (19)

JHEP06(2025)086

	Equal binning scheme		Optimal binning scheme		Modified optimal binning scheme	
Bin	F_i	F'_i	F_i	F'_i	F_i	F'_i
-8	0.028 ± 0.001	0.036 ± 0.001	0.064 ± 0.002	0.063 ± 0.001	0.054 ± 0.001	0.054 ± 0.001
-7	0.013 ± 0.001	0.017 ± 0.001	0.052 ± 0.002	0.061 ± 0.001	0.044 ± 0.001	0.046 ± 0.001
-6	0.014 ± 0.001	0.012 ± 0.001	0.004 ± 0.001	0.008 ± 0.001	0.011 ± 0.001	0.017 ± 0.001
-5	0.052 ± 0.002	0.042 ± 0.001	0.031 ± 0.001	0.030 ± 0.001	0.026 ± 0.001	0.025 ± 0.001
-4	0.016 ± 0.001	0.014 ± 0.001	0.064 ± 0.002	0.051 ± 0.001	0.052 ± 0.001	0.043 ± 0.001
-3	0.020 ± 0.001	0.022 ± 0.001	0.004 ± 0.001	0.009 ± 0.001	0.019 ± 0.001	0.028 ± 0.001
-2	0.018 ± 0.001	0.024 ± 0.001	0.004 ± 0.001	0.014 ± 0.001	0.020 ± 0.001	0.037 ± 0.001
-1	0.081 ± 0.002	0.093 ± 0.002	0.020 ± 0.001	0.022 ± 0.001	0.015 ± 0.001	0.011 ± 0.001
1	0.174 ± 0.003	0.177 ± 0.003	0.097 ± 0.002	0.092 ± 0.002	0.051 ± 0.002	0.049 ± 0.001
2	0.086 ± 0.002	0.083 ± 0.002	0.143 ± 0.003	0.142 ± 0.002	0.163 ± 0.003	0.171 ± 0.002
3	0.067 ± 0.002	0.064 ± 0.001	0.144 ± 0.003	0.141 ± 0.002	0.225 ± 0.004	0.218 ± 0.003
4	0.025 ± 0.001	0.026 ± 0.001	0.109 ± 0.002	0.103 ± 0.002	0.088 ± 0.002	0.081 ± 0.001
5	0.087 ± 0.002	0.080 ± 0.001	0.052 ± 0.001	0.054 ± 0.001	0.037 ± 0.001	0.039 ± 0.001
6	0.060 ± 0.002	0.059 ± 0.001	0.074 ± 0.002	0.070 ± 0.001	0.079 ± 0.002	0.076 ± 0.001
7	0.127 ± 0.003	0.122 ± 0.002	0.117 ± 0.002	0.120 ± 0.002	0.091 ± 0.002	0.086 ± 0.002
8	0.133 ± 0.003	0.130 ± 0.002	0.023 ± 0.001	0.021 ± 0.001	0.024 ± 0.001	0.022 ± 0.001

Table 3. The averaged $F_i^{(\prime)}$ values for the three binning schemes, where the uncertainties are only statistical.

from ref. [14], incorporating the updated strong-phase parameters [35, 36] and amplitude models [16, 33]. Furthermore, the binned fractional signal yields $F_i^{(\prime)} = \frac{K_i^{(\prime)}}{\sum_j K_j^{(\prime)}}$ for each flavour tag are determined. As demonstrated in figure 6, these yields are in good agreement across bins. The averaged $F_i^{(\prime)}$ values are summarized in table 3.

5.2 Expected number of binned signal events

Following eqs. (2.3) and (2.7), the binned signal yields of the $K^0_{S/L}\pi^+\pi^-$ decays tagged by *CP* eigenstates are expressed in terms of the ST yields and reconstruction efficiencies as

$$\begin{aligned} M_i &= h_{CP} \sum_{j=1}^{8} \epsilon_{ij} \left(K_j + K_{-j} - (2F_{CP}^{+} - 1) \times 2c_j \sqrt{K_j K_{-j}} \right), \\ M'_i &= h'_{CP} \sum_{j=1}^{8} \epsilon'_{ij} \left(K'_j + K'_{-j} + (2F_{CP}^{+} - 1) \times 2c'_j \sqrt{K'_j K'_{-j}} \right). \end{aligned} \tag{5.1}$$

Here, the normalization factor $h_{CP}^{(\prime)}$ is determined by the ratio of the efficiency-corrected ST yields of the *CP* eigenstates to those of the flavour modes, given by $S_{CP}/S_F^{(\prime)}$. To accurately account for the DCS contributions and charm mixing effects in the ST yields, S_{CP} is corrected with the factor of $(1 - (2F_{CP}^{+} - 1)y + y^2)$ and $S_F^{(\prime)}$ is corrected with $(1 + (r_D^F)^2 - 2yR_F r_D^F \cos\delta_D^F + y^2)$. Here, r_D^F, R_F and δ_D^F are the decay parameters in the three hadronic flavour tags as determined in refs. [35, 36]. The charm mixing parameter y is equal to $(0.647 \pm 0.024)\%$ according to ref. [36].

JHEP06(2025)086

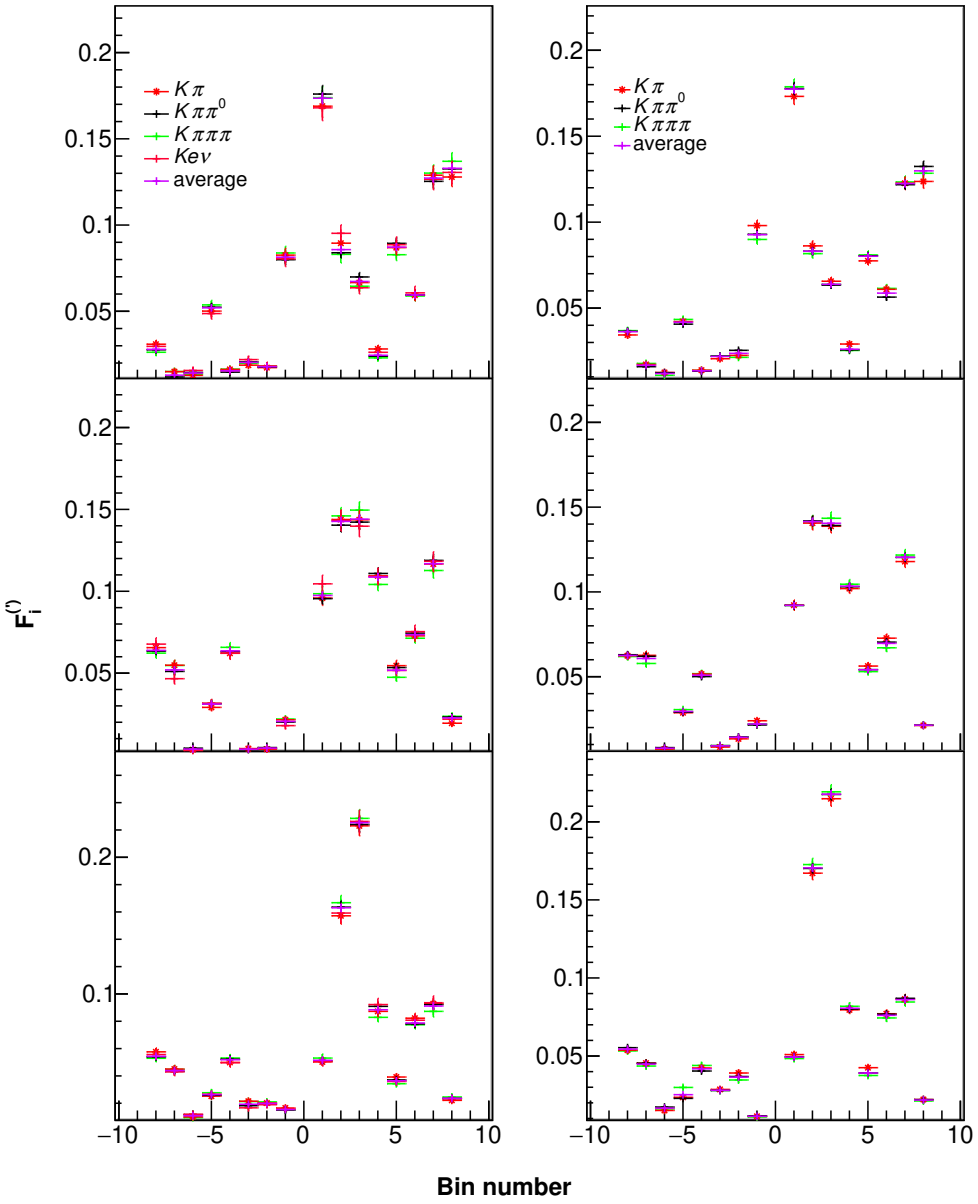

Figure 6. The $F_i^{(\prime)}$ distribution for the $K^0_S\pi^+\pi^-$ decay (left) and the $K^0_L\pi^+\pi^-$ decay (right) under the equal binning scheme (top), the optimal binning scheme (middle) and the modified optimal binning scheme (bottom). The different colors represent the $F_i^{(\prime)}$ results of different tags and the averaged values.

For the DT $K^0_S\pi^+\pi^-$ versus $K^0_S\pi^+\pi^-$, there are 72 observables due to the symmetry of the Dalitz plot. In contrast, the DT $K^0_S\pi^+\pi^-$ versus $K^0_L\pi^+\pi^-$ involves 128 observables. The expected signal yields are expressed as

$$\begin{aligned} M_{ij} &= h_{\rm corr} \sum_{m\to(i,j)=0}^{m=72} \epsilon_{mn}\left(K_iK_{-j}+K_{-i}K_j-2\sqrt{K_iK_{-i}K_jK_{-j}}(c_ic_j+s_is_j)\right), \\ M'_{ij} &= h'_{\rm corr} \sum_{m\to(i,j)=0}^{m=128} \epsilon'_{mn}\left(K_iK'_{-j}+K_{-i}K'_j+2\sqrt{K_iK_{-i}K'_jK'_{-j}}(c_ic'_j+s_is'_j)\right). \end{aligned} \tag{5.2}$$

JHEP06(2025)086

Here, the normalization factors are given by $h_{\rm corr} = \frac{N_{D^0\bar{D}^0}}{S^2_{\rm flav}} \times \alpha\beta$ and $h'_{\rm corr} = \frac{2N_{D^0\bar{D}^0}}{S_{\rm flav}S'_{\rm flav}}$. The parameter α is determined from the symmetry of Dalitz plots and is 1 for the bin pair (i, j) where $|i| = |j|$ and 2 otherwise. $\beta = \frac{2Br(K^0_S\to\pi^0\pi^0)}{Br(K^0_S\to\pi^+\pi^-)}$ when one K^0_S is reconstructed with the decay $\pi^0\pi^0$. Here, $Br(K^0_S \to \pi^0\pi^0)$ and $Br(K^0_S \to \pi^+\pi^-)$ are the branching fractions of $K^0_S \to \pi^0\pi^0$ and $K^0_S \to \pi^+\pi^-$. The total number of $D^0\bar{D}^0$ pairs $N_{D^0\bar{D}^0}$ is estimated to be $(28660 \pm 247) \times 10^3$ for the utilized data set [15].

5.3 Fit to the $c_i^{(\prime)}$ and $s_i^{(\prime)}$ parameters

The strong-phase difference parameters $c_i^{(\prime)}$ and $s_i^{(\prime)}$ are determined via a maximum likelihood fit to the observed and expected numbers of signal events. Under the assumption that the sum of binned signal yields and peaking background follows a Poisson distribution, the likelihood function is formulated as

$$\begin{aligned} -2\ln\mathscr{L} = & -2\sum_{i=1}^{8}\ln(\text{Poisson}(N_i^{\rm obs}, N_i^{\rm exp})_{K^0_{S/L}\pi^+\pi^-\ \text{versus}\ CP}) \\ & -2\sum_{i=1}^{72}\ln(\text{Poisson}(N_i^{\rm obs}, N_i^{\rm exp})_{K^0_S\pi^+\pi^-\ \text{versus}\ K^0_S\pi^+\pi^-}) \\ & -2\sum_{i=1}^{128}\ln(\text{Poisson}(N_i^{\rm obs}, N_i^{\rm exp})_{K^0_S\pi^+\pi^-\ \text{versus}\ K^0_L\pi^+\pi^-}). \end{aligned} \tag{5.3}$$

Here, $N_i^{\rm exp}$ represents the sum of the expected signal yields $M_i^{(\prime)}$ and the peaking background contributions. However, since the non-peaking background in the $K^0_L\pi^+\pi^-$ versus $\pi^+\pi^-\pi^0$ mode is significantly larger than that in other modes, the number of non-peaking background events is added to $N_i^{\rm exp}$. To avoid large statistical fluctuations, self-conjugated tags $K^0_S\pi^+\pi^-$, $K^0_S(\pi)_{\rm miss}\pi$, $(\pi^0(\pi^0)_{\rm miss})_{K^0_S}\pi\pi$ are combined. For CP tags, $K^0_S\eta_{\gamma\gamma}$ and $K^0_S\eta_{\pi^+\pi^-\pi^0}$ tags are combined similarly, and $K^0_S\eta'_{\gamma\rho}$ and $K^0_S\eta'_{\pi\pi\eta}$ tags are also combined. The results of the model-independent fits to $c_i^{(\prime)}$ and $s_i^{(\prime)}$ parameters under the three binning schemes are listed in table 4. Discussions on systematic uncertainties are presented in the next section. The correlation matrices of statistical uncertainties are shown in tables 14–16 in appendix D.

Model-predicted differences in the strong-phase parameters between $K^0_S\pi^+\pi^-$ and $K^0_L\pi^+\pi^-$ decays, denoted as Δc_i and Δs_i, have been used to improve the precision of the $c_i^{(\prime)}$ and $s_i^{(\prime)}$ parameters [14]. Using the amplitude model of the $K^0_S\pi^+\pi^-$ decay [33] and the U-spin breaking parameters for the $K^0_L\pi^+\pi^-$ decay [16], the model-predicted Δc_i and Δs_i parameters have been updated, as detailed in table 6 in appendix A. The differences between the $K^0_S\pi^+\pi^-$ amplitude models measured by the Belle and BESIII experiments [16, 33] and the uncertainties of the U-spin breaking parameters are assigned as their uncertainties. The Δc_i and Δs_i parameters determined by the unconstrained c_i and s_i results, which are consistent with the model-predicted parameters within 2σ, are shown in table 7 in appendix A. To incorporate these constraints into the likelihood fit, a χ^2 term as follows is added to the likelihood function in eq. (5.3)

$$\chi^2 = \frac{(c'_i - c_i - \Delta c_i)^2}{\sigma^2_{\Delta c_i}} + \frac{(s'_i - s_i - \Delta s_i)^2}{\sigma^2_{\Delta s_i}}. \tag{5.4}$$

JHEP06(2025)086

Bin	c_i	s_i	c_i'	s_i'
		Equal binning scheme		
1	$0.682 \pm 0.017 \pm 0.008$	$-0.007 \pm 0.052 \pm 0.006$	$0.755 \pm 0.018 \pm 0.009$	$0.025 \pm 0.087 \pm 0.006$
2	$0.602 \pm 0.035 \pm 0.013$	$0.270 \pm 0.120 \pm 0.022$	$0.668 \pm 0.034 \pm 0.012$	$0.557 \pm 0.143 \pm 0.018$
3	$0.060 \pm 0.034 \pm 0.009$	$0.666 \pm 0.088 \pm 0.015$	$0.265 \pm 0.034 \pm 0.007$	$1.031 \pm 0.150 \pm 0.018$
4	$-0.553 \pm 0.043 \pm 0.012$	$0.681 \pm 0.123 \pm 0.023$	$-0.575 \pm 0.045 \pm 0.008$	$0.722 \pm 0.196 \pm 0.030$
5	$-0.955 \pm 0.017 \pm 0.007$	$-0.117 \pm 0.056 \pm 0.005$	$-0.923 \pm 0.020 \pm 0.010$	$-0.148 \pm 0.118 \pm 0.010$
6	$-0.574 \pm 0.043 \pm 0.014$	$-0.431 \pm 0.110 \pm 0.018$	$-0.343 \pm 0.047 \pm 0.010$	$-0.604 \pm 0.214 \pm 0.033$
7	$0.072 \pm 0.045 \pm 0.014$	$-0.810 \pm 0.102 \pm 0.018$	$0.313 \pm 0.043 \pm 0.011$	$-0.717 \pm 0.183 \pm 0.036$
8	$0.522 \pm 0.030 \pm 0.011$	$-0.363 \pm 0.080 \pm 0.010$	$0.609 \pm 0.032 \pm 0.011$	$-0.352 \pm 0.134 \pm 0.020$
		Optimal binning scheme		
1	$0.034 \pm 0.036 \pm 0.011$	$-0.741 \pm 0.090 \pm 0.015$	$0.179 \pm 0.036 \pm 0.007$	$-0.686 \pm 0.155 \pm 0.029$
2	$0.946 \pm 0.066 \pm 0.034$	$-0.116 \pm 0.179 \pm 0.033$	$0.823 \pm 0.044 \pm 0.021$	$0.129 \pm 0.167 \pm 0.024$
3	$0.244 \pm 0.078 \pm 0.025$	$-0.622 \pm 0.168 \pm 0.030$	$0.613 \pm 0.053 \pm 0.024$	$-0.390 \pm 0.200 \pm 0.035$
4	$-0.909 \pm 0.016 \pm 0.008$	$-0.195 \pm 0.053 \pm 0.006$	$-0.869 \pm 0.018 \pm 0.010$	$-0.258 \pm 0.097 \pm 0.015$
5	$-0.215 \pm 0.031 \pm 0.010$	$0.883 \pm 0.083 \pm 0.016$	$-0.150 \pm 0.031 \pm 0.005$	$0.906 \pm 0.127 \pm 0.020$
6	$0.342 \pm 0.071 \pm 0.021$	$0.566 \pm 0.185 \pm 0.039$	$0.646 \pm 0.053 \pm 0.022$	$0.911 \pm 0.204 \pm 0.033$
7	$0.871 \pm 0.017 \pm 0.008$	$0.128 \pm 0.071 \pm 0.011$	$0.875 \pm 0.019 \pm 0.010$	$0.186 \pm 0.088 \pm 0.007$
8	$0.845 \pm 0.025 \pm 0.011$	$-0.197 \pm 0.096 \pm 0.012$	$0.801 \pm 0.029 \pm 0.013$	$-0.083 \pm 0.139 \pm 0.021$
		Modified optimal binning scheme		
1	$-0.283 \pm 0.044 \pm 0.012$	$-0.276 \pm 0.128 \pm 0.020$	$-0.180 \pm 0.049 \pm 0.006$	$-0.239 \pm 0.188 \pm 0.035$
2	$0.828 \pm 0.029 \pm 0.016$	$-0.042 \pm 0.094 \pm 0.017$	$0.860 \pm 0.024 \pm 0.012$	$0.036 \pm 0.098 \pm 0.015$
3	$0.098 \pm 0.034 \pm 0.016$	$-0.687 \pm 0.082 \pm 0.015$	$0.389 \pm 0.028 \pm 0.010$	$-0.507 \pm 0.117 \pm 0.022$
4	$-0.965 \pm 0.016 \pm 0.006$	$-0.195 \pm 0.060 \pm 0.006$	$-0.894 \pm 0.020 \pm 0.010$	$-0.134 \pm 0.113 \pm 0.012$
5	$-0.427 \pm 0.034 \pm 0.010$	$0.845 \pm 0.102 \pm 0.019$	$-0.473 \pm 0.034 \pm 0.005$	$0.800 \pm 0.150 \pm 0.020$
6	$0.241 \pm 0.043 \pm 0.013$	$0.730 \pm 0.114 \pm 0.019$	$0.516 \pm 0.037 \pm 0.015$	$0.937 \pm 0.154 \pm 0.026$
7	$0.727 \pm 0.022 \pm 0.010$	$0.109 \pm 0.090 \pm 0.011$	$0.713 \pm 0.025 \pm 0.010$	$0.272 \pm 0.115 \pm 0.011$
8	$0.786 \pm 0.027 \pm 0.010$	$-0.201 \pm 0.103 \pm 0.012$	$0.729 \pm 0.030 \pm 0.013$	$-0.148 \pm 0.145 \pm 0.021$

Table 4. The $c_i^{(\prime)}$ and $s_i^{(\prime)}$ parameters determined from the model-independent measurement under three binning schemes. The first uncertainties are statistical and the second are systematic.

The fit results incorporating the model-predicted Δc_i and Δs_i constraints are summarized in table 5. The correlation matrices of statistical uncertainties are shown in tables 20–22 in appendix D. Compared to the unconstrained c_i and s_i results, the constrained c_i and s_i results are closer to the model-prediction with a significantly smaller uncertainty. Both sets of results are consistent within 2σ as illustrated in figure 7. The constrained results are consistent with the previous BESIII measurement [14] within 2σ.

5.4 Systematic uncertainties

The dominant sources of systematic uncertainties are identified as follows: statistical fluctuations in the $K_i^{(\prime)}$ parameters, inputs of the hadronic parameters for flavour tags and charm

JHEP06(2025)086

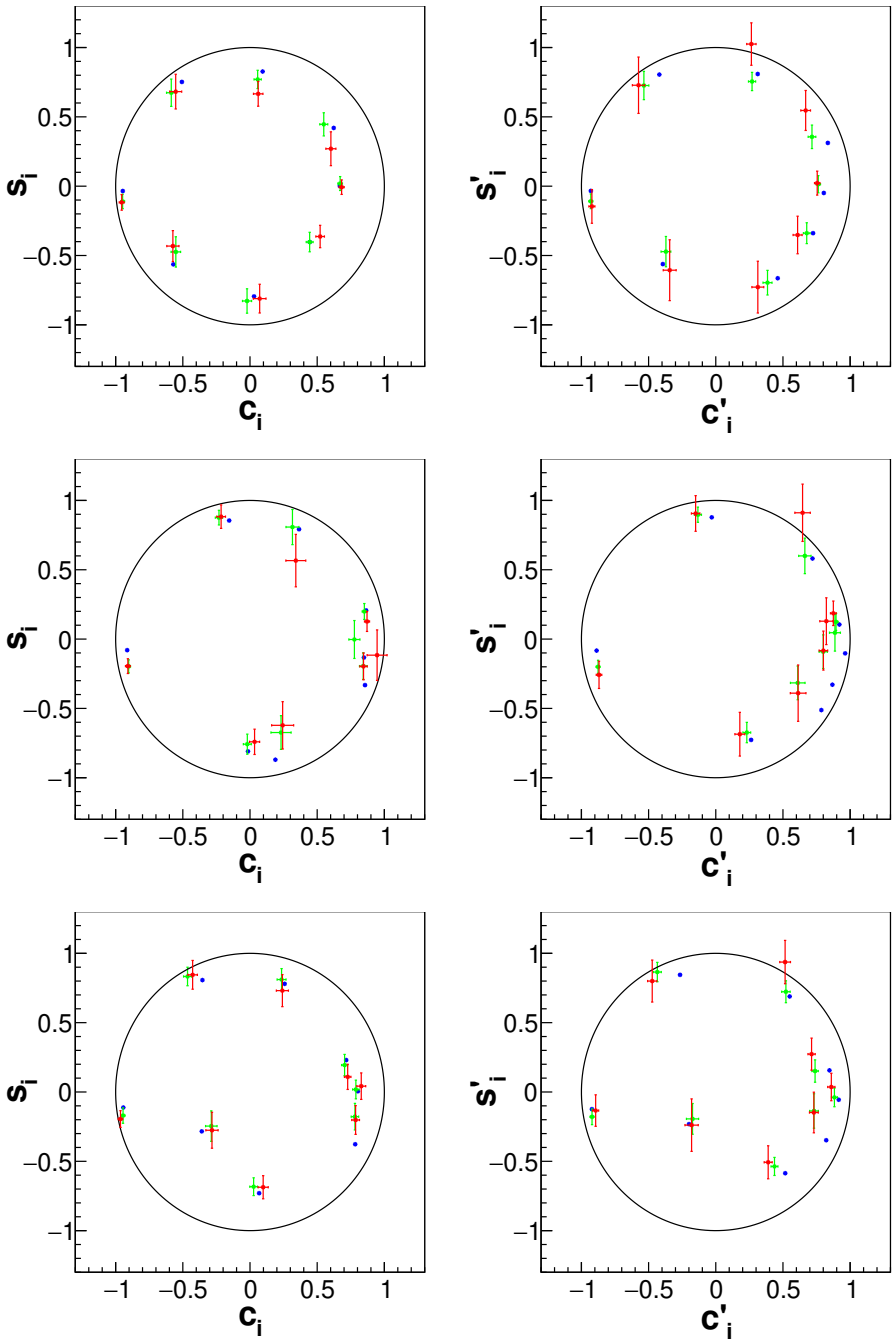

Figure 7. The $c_i^{(\prime)}/s_i^{(\prime)}$ parameters determined without constraints (red), with constraints (green) and predicted by the amplitude models [33] (blue) under the equal binning scheme (top), the optimal binning scheme (middle) and the modified optimal binning scheme (bottom).

mixing parameters, statistical fluctuations in the ST yields, limited statistics of the signal MC samples, and background estimation.

To determine these uncertainties, pseudo-experiments are performed. Specifically, 1000 sets of values for the $K_i^{(\prime)}$ parameters, input parameters, ST yields, signal efficiencies, and background contributions are generated individually from Gaussian distributions. These

JHEP06(2025)086

Bin	c_i	s_i	c'_i	s'_i
Equal binning scheme				
1	$0.671 \pm 0.015 \pm 0.008$	$0.019 \pm 0.050 \pm 0.004$	$0.763 \pm 0.015 \pm 0.007$	$0.014 \pm 0.061 \pm 0.004$
2	$0.549 \pm 0.028 \pm 0.010$	$0.446 \pm 0.082 \pm 0.009$	$0.716 \pm 0.027 \pm 0.010$	$0.356 \pm 0.083 \pm 0.010$
3	$0.056 \pm 0.026 \pm 0.007$	$0.770 \pm 0.064 \pm 0.010$	$0.270 \pm 0.026 \pm 0.006$	$0.754 \pm 0.065 \pm 0.010$
4	$-0.586 \pm 0.034 \pm 0.009$	$0.674 \pm 0.097 \pm 0.011$	$-0.535 \pm 0.036 \pm 0.007$	$0.726 \pm 0.101 \pm 0.015$
5	$-0.948 \pm 0.013 \pm 0.007$	$-0.110 \pm 0.052 \pm 0.004$	$-0.930 \pm 0.014 \pm 0.007$	$-0.109 \pm 0.053 \pm 0.004$
6	$-0.552 \pm 0.034 \pm 0.010$	$-0.474 \pm 0.107 \pm 0.016$	$-0.371 \pm 0.035 \pm 0.009$	$-0.472 \pm 0.108 \pm 0.016$
7	$-0.023 \pm 0.032 \pm 0.011$	$-0.827 \pm 0.087 \pm 0.013$	$0.385 \pm 0.032 \pm 0.009$	$-0.696 \pm 0.088 \pm 0.012$
8	$0.444 \pm 0.024 \pm 0.009$	$-0.402 \pm 0.070 \pm 0.007$	$0.677 \pm 0.024 \pm 0.009$	$-0.339 \pm 0.075 \pm 0.007$
Optimal binning scheme				
1	$-0.020 \pm 0.028 \pm 0.009$	$-0.758 \pm 0.071 \pm 0.014$	$0.231 \pm 0.028 \pm 0.007$	$-0.674 \pm 0.072 \pm 0.014$
2	$0.777 \pm 0.037 \pm 0.021$	$-0.003 \pm 0.136 \pm 0.014$	$0.887 \pm 0.036 \pm 0.019$	$0.046 \pm 0.132 \pm 0.014$
3	$0.231 \pm 0.071 \pm 0.024$	$-0.674 \pm 0.120 \pm 0.019$	$0.610 \pm 0.050 \pm 0.021$	$-0.316 \pm 0.120 \pm 0.019$
4	$-0.903 \pm 0.012 \pm 0.007$	$-0.197 \pm 0.047 \pm 0.005$	$-0.876 \pm 0.013 \pm 0.007$	$-0.200 \pm 0.047 \pm 0.005$
5	$-0.231 \pm 0.026 \pm 0.007$	$0.876 \pm 0.052 \pm 0.009$	$-0.133 \pm 0.026 \pm 0.005$	$0.897 \pm 0.054 \pm 0.009$
6	$0.316 \pm 0.045 \pm 0.017$	$0.808 \pm 0.123 \pm 0.031$	$0.663 \pm 0.043 \pm 0.016$	$0.600 \pm 0.124 \pm 0.032$
7	$0.851 \pm 0.014 \pm 0.008$	$0.199 \pm 0.057 \pm 0.006$	$0.895 \pm 0.013 \pm 0.008$	$0.124 \pm 0.061 \pm 0.005$
8	$0.843 \pm 0.025 \pm 0.011$	$-0.195 \pm 0.095 \pm 0.012$	$0.800 \pm 0.028 \pm 0.013$	$-0.091 \pm 0.120 \pm 0.018$
Modified optimal binning scheme				
1	$-0.288 \pm 0.041 \pm 0.012$	$-0.246 \pm 0.109 \pm 0.013$	$-0.174 \pm 0.045 \pm 0.006$	$-0.193 \pm 0.110 \pm 0.014$
2	$0.788 \pm 0.021 \pm 0.012$	$0.018 \pm 0.067 \pm 0.007$	$0.882 \pm 0.020 \pm 0.010$	$-0.039 \pm 0.067 \pm 0.007$
3	$0.026 \pm 0.025 \pm 0.014$	$-0.682 \pm 0.063 \pm 0.012$	$0.437 \pm 0.024 \pm 0.009$	$-0.537 \pm 0.064 \pm 0.012$
4	$-0.945 \pm 0.013 \pm 0.007$	$-0.170 \pm 0.055 \pm 0.008$	$-0.921 \pm 0.013 \pm 0.007$	$-0.179 \pm 0.056 \pm 0.008$
5	$-0.465 \pm 0.028 \pm 0.009$	$0.833 \pm 0.066 \pm 0.010$	$-0.435 \pm 0.029 \pm 0.005$	$0.865 \pm 0.069 \pm 0.010$
6	$0.235 \pm 0.031 \pm 0.012$	$0.811 \pm 0.077 \pm 0.017$	$0.522 \pm 0.030 \pm 0.010$	$0.722 \pm 0.077 \pm 0.018$
7	$0.704 \pm 0.021 \pm 0.008$	$0.194 \pm 0.076 \pm 0.012$	$0.739 \pm 0.022 \pm 0.009$	$0.151 \pm 0.080 \pm 0.009$
8	$0.781 \pm 0.026 \pm 0.010$	$-0.177 \pm 0.095 \pm 0.013$	$0.731 \pm 0.030 \pm 0.012$	$-0.137 \pm 0.123 \pm 0.018$

Table 5. The $c_i^{(\prime)}$ and $s_i^{(\prime)}$ parameters constrained by Δc_i and Δs_i parameters under three binning schemes. The first uncertainties are statistical and the second are systematic.

distributions have means equal to the nominal parameter values and standard deviations reflecting their respective uncertainties.

For each set of generated values, the likelihood fit to obtain the $c_i^{(\prime)}$ and $s_i^{(\prime)}$ parameters is repeated for each uncertainty contribution. No significant bias is observed in the re-fitted $c_i^{(\prime)}$ and $s_i^{(\prime)}$ parameters. The standard deviations of the resultant distributions are taken as the corresponding systematic uncertainties.

Most of the systematic uncertainties associated with the PID and tracking efficiencies are found to be negligible. This is due to the corrections from control samples having been applied to the K_S^0 selection efficiency and the tracking and PID efficiencies of π's not originating from K_S^0. However, the tracking efficiencies of π's coming from K_S^0 introduce a non-negligible uncertainty. The signal efficiencies are varied by the tracking efficiency corrections estimated

JHEP06(2025)086

with $\pi^{\pm}$ control samples. The differences between the nominal and refitted $c_i^{(\prime)}$ and $s_i^{(\prime)}$ parameters are then taken as the systematic uncertainties.

The above systematic uncertainties are determined separately for both the constrained and unconstrained $c_i^{(\prime)}$ and $s_i^{(\prime)}$ results under three different binning schemes, details of which can be found in tables 8–13 appendix C. The correlation matrices of the systematic uncertainties, derived from the pseudo-experiments, are detailed in tables 17–19 and 23–25 in appendix D.

6 Impact of the results on the γ measurement

The decay mode $B^- \to DK^-$, with $D \to K^0_S\pi^+\pi^-$ gives the most precise model-independent angle γ measurement channel, where the γ is determined through comparing the expected and observed binned yields of B decay. The expected binned yield of $B^- \to DK^-$, $D \to K^0_S\pi^+\pi^-$ [6] is calculated using the input parameters of c_i, s_i and F_i from D decays and the parameters γ, δ_B, r_B from B decays, which are formulated as

$$\begin{aligned}
N_i^{\rm exp}(B^- \to K^-D) &= h_B^-[F_i + r_B^2 F_{-i} + 2r_B\sqrt{F_iF_{-i}} \times c_i\cos(\delta_B - \gamma) - s_i\sin(\delta_B - \gamma)],\\
N_{-i}^{\rm exp}(B^- \to K^-D) &= h_B^-[F_{-i} + r_B^2 F_i + 2r_B\sqrt{F_iF_{-i}} \times c_i\cos(\delta_B - \gamma) + s_i\sin(\delta_B - \gamma)],\\
N_i^{\rm exp}(B^+ \to K^+D) &= h_B^+[F_{-i} + r_B^2 F_i + 2r_B\sqrt{F_iF_{-i}} \times c_i\cos(\delta_B + \gamma) + s_i\sin(\delta_B + \gamma)],\\
N_{-i}^{\rm exp}(B^+ \to K^+D) &= h_B^+[F_i + r_B^2 F_{-i} + 2r_B\sqrt{F_iF_{-i}} \times c_i\cos(\delta_B + \gamma) - s_i\sin(\delta_B + \gamma)].
\end{aligned} \tag{6.1}$$

To evaluate the impact of the strong-phase parameters (c_i, s_i) on the measurement of γ, a large simulated dataset of B decays is generated by setting the input parameters to $\gamma = 68.7^\circ$, $r_B = 0.0904$, $\delta_B = 118.3^\circ$ [9], and the measured c_i, s_i, F_i. The normalization factor h_B is set to be a large number to suppress the influence of B decay statistics. Then, 1000 toy samples of c_i and s_i parameters are generated by sampling according to their uncertainties and correlations. For each toy sample of generated c_i and s_i parameters, the γ values are fitted using the pseudo-data binned yields of B decays, the measured F_i parameters as well as the toy c_i and s_i parameters. The standard deviation of the resulting γ value is taken as the uncertainty contribution of the strong-phase parameters.

The uncertainties contributed by the constrained and unconstrained strong-phase parameters to the γ measurement in the optimal binning scheme are found to be 0.9° and 1.5°, respectively, as shown in figure 8. Furthermore, the difference of the γ mean value by taking the constrained and unconstrained strong-phase parameters as input is found to be around 0.4° for the optimal binning scheme. The uncertainty contributions under the equal binning scheme and modified optimal binning scheme are also studied, which are $0.7^\circ(0.9^\circ)$ and $0.8^\circ(1.1^\circ)$ by taking the (un)constrained strong-phase parameters as inputs. The difference of the γ angles by taking the constrained and unconstrained strong-phase parameters as inputs are found to be 0.3° for the equal binning scheme and 0.4° for the modified binning scheme. Furthermore, the updated result can provide better input for the γ measurement in the upcoming B factory upgrades [37, 38] and will not become the dominant source of uncertainty.

7 Summary

An improved measurement of the strong-phase parameters between D^0 and $\bar{D}^0 \to K^0_{S/L}\pi^+\pi^-$ decays has been preformed using BESIII $\psi(3770)$ dataset of $7.93\,\text{fb}^{-1}$. The $c_i^{(\prime)}$ and $s_i^{(\prime)}$

JHEP06(2025)086

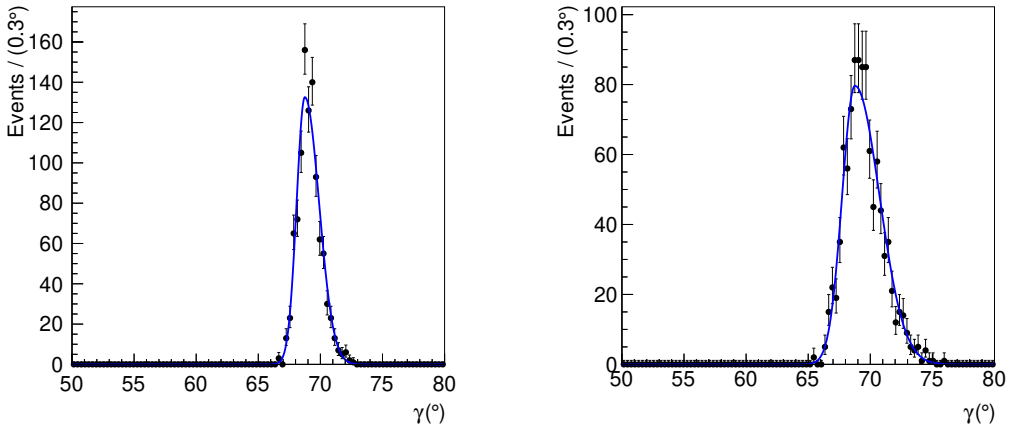

Figure 8. The impact on the γ measurement for the optimal binning scheme with (left) and without (right) constraints.

parameters have been measured with or without the constraints of model-predicted differences between the strong-phase parameters in the $D^0 \to K^0_{S/L}\pi^+\pi^-$ decays. These results provide essential inputs for the angle γ measurement at LHCb and Belle. The propagated uncertainty from the constrained strong-phase inputs contributing to the γ measurement is found to be 0.9° based on optimal binning scheme, where it is 1.5° from the unconstrained result. In this case, constraints in the strong-phase parameters are found to have a negligible effect on the current γ measurement at LHCb and Belle, which has the best statistical uncertainty of about 5° [9].

Acknowledgments

The BESIII collaboration thanks the staff of BEPCII (https://cstr.cn/31109.02.BEPC) and the IHEP computing center for their strong support. This work is supported in part by National Key R&D Program of China under Contracts Nos. 2023YFA1606000, 2023YFA1606704; National Natural Science Foundation of China (NSFC) under Contracts Nos. 11635010, 11935015, 11935016, 11935018, 12025502, 12035009, 12035013, 12061131003, 12192260, 12192261, 12192262, 12192263, 12192264, 12192265, 12221005, 12225509, 12235017, 12361141819, 12405112; the Chinese Academy of Sciences (CAS) Large-Scale Scientific Facility Program; CAS under Contract No. YSBR-101; 100 Talents Program of CAS; The Institute of Nuclear and Particle Physics (INPAC) and Shanghai Key Laboratory for Particle Physics and Cosmology; Agencia Nacional de Investigación y Desarrollo de Chile (ANID), Chile under Contract No. ANID PIA/APOYO AFB230003; German Research Foundation DFG under Contract No. FOR5327; Istituto Nazionale di Fisica Nucleare, Italy; Knut and Alice Wallenberg Foundation under Contracts Nos. 2021.0174, 2021.0299; Ministry of Development of Turkey under Contract No. DPT2006K-120470; National Research Foundation of Korea under Contract No. NRF-2022R1A2C1092335; National Science and Technology fund of Mongolia; National Science Research and Innovation Fund (NSRF) via the Program Management Unit for Human Resources & Institutional Development, Research and Innovation of Thailand under Contract No. B50G670107; Polish National Science Centre under Contract No. 2024/53/B/ST2/00975; Swedish Research Council under Contract No. 2019.04595; U.S. Department of Energy under Contract No. DE-FG02-05ER41374.

JHEP06(2025)086

A Fitting plots in logarithmic scale

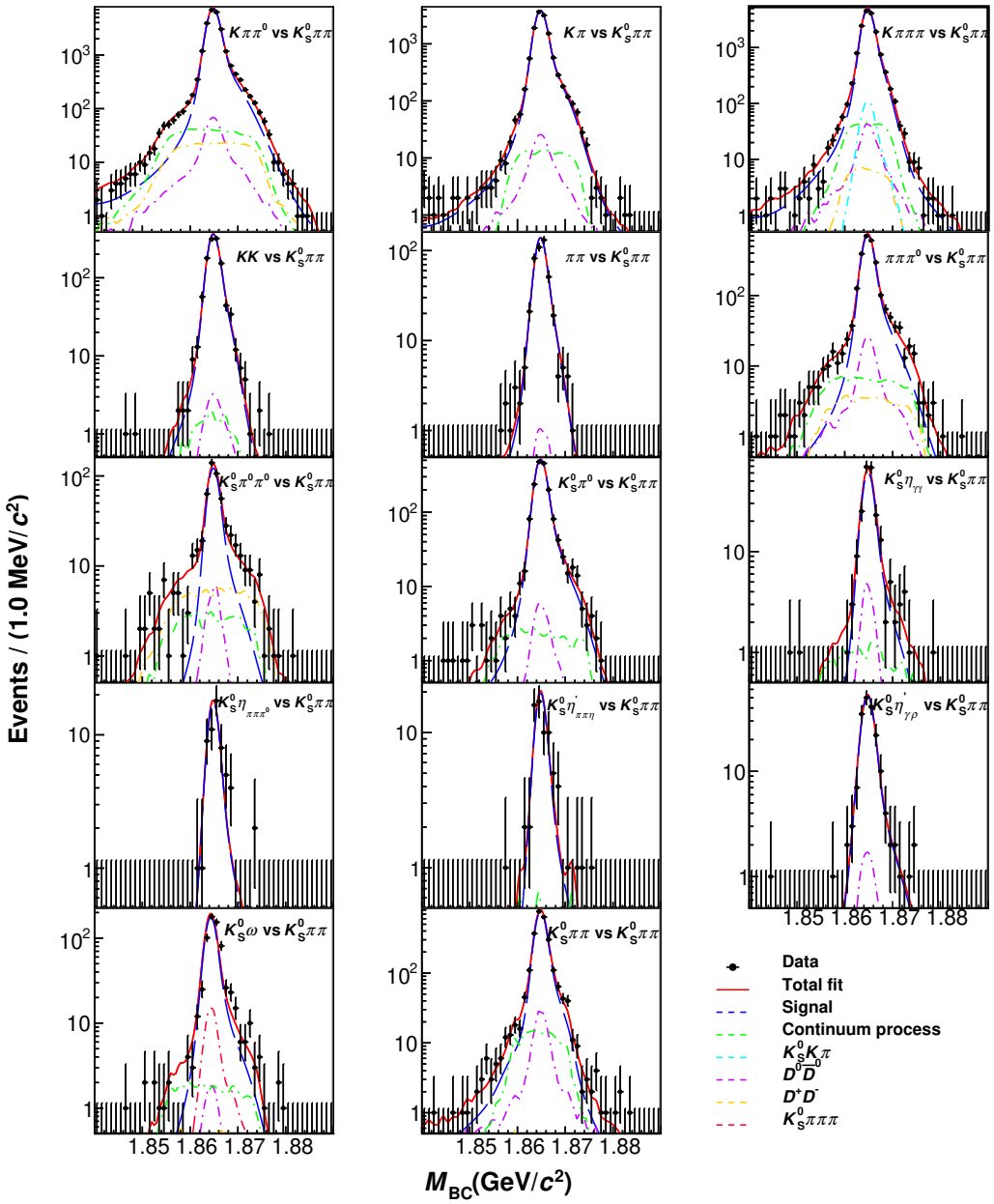

Figure 9. The logarithmic scale 1D unbinned maximum likelihood fits for $K^0_S\pi^+\pi^-$ versus full reconstructed modes on $M_{\rm BC}$. The black points with error bars represent data. The dashed lines indicate the signal and background shapes. The red lines represent the sum of signal and background shapes.

JHEP06(2025)086

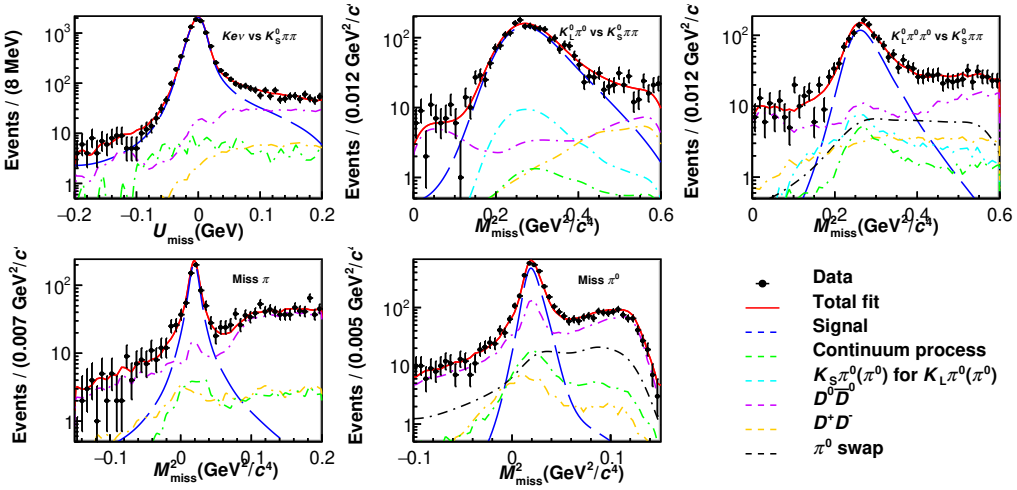

Figure 10. The logarithmic scale 1D unbinned maximum likelihood fits for $K^0_S\pi^+\pi^-$ versus partially reconstructed tags on $M^2_{\rm miss}/U_{\rm miss}$. The black points with error bars represent data. The dashed lines indicate the signal and background shapes. The red lines represent the sum of signal and background shapes.

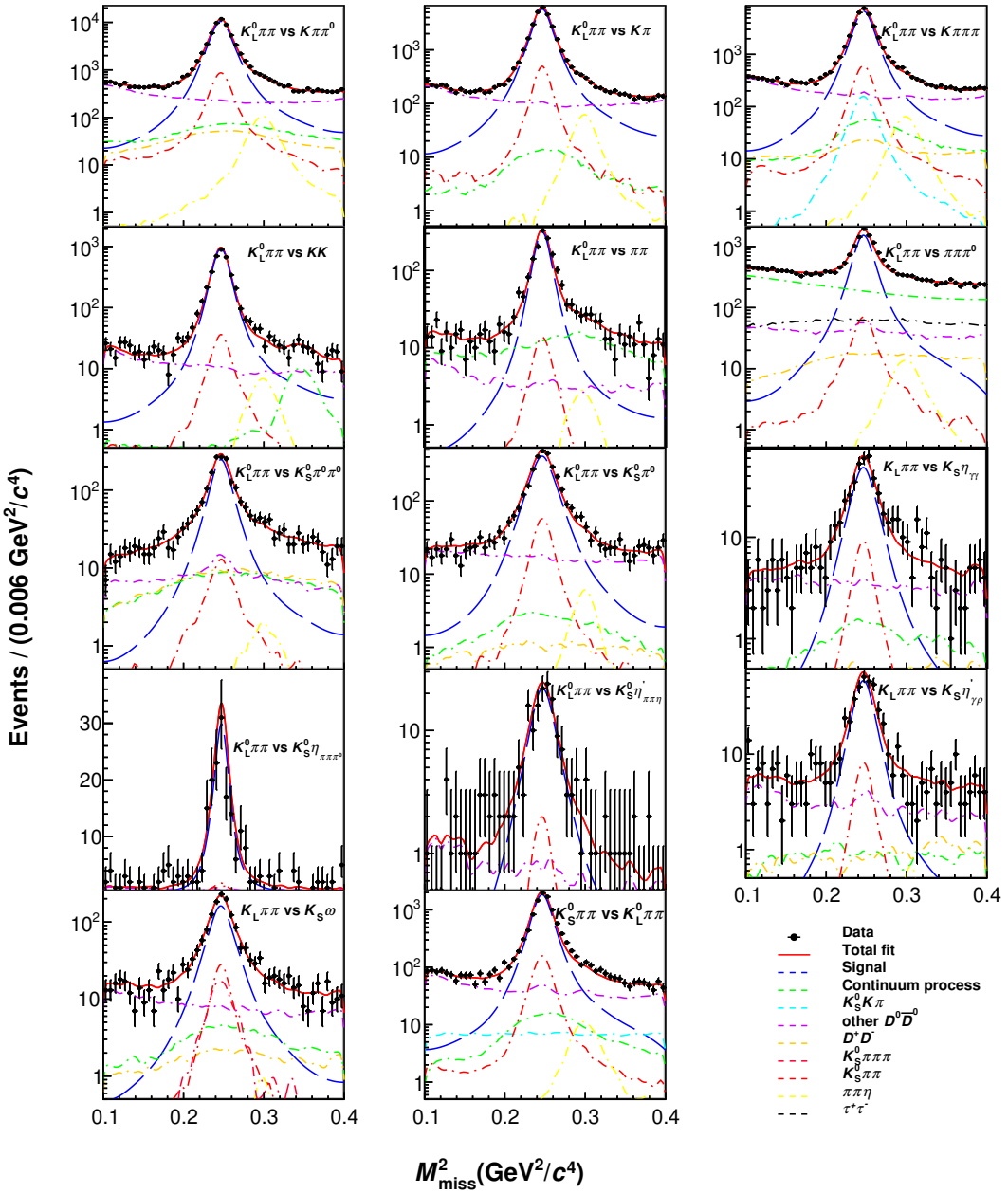

Figure 11. The logarithmic scale 1D unbinned maximum likelihood fits for $K_L^0\pi^+\pi^-$ versus various tag modes on $M^2_{\rm miss}$. The black points with error bars represent data. The dashed lines indicate the signal and background shapes. The red lines represent the sum of signal and background shapes.

JHEP06(2025)086

B Values of Δc_i and Δs_i constraints

Bin	Δc_i	Δs_i	Δc_i	Δs_i	Δc_i	Δs_i
	Equal		Optimal		Modified optimal	
1	0.136 ± 0.024	-0.051 ± 0.085	0.278 ± 0.025	0.083 ± 0.014	0.160 ± 0.102	0.052 ± 0.032
2	0.211 ± 0.031	-0.108 ± 0.043	0.115 ± 0.011	0.030 ± 0.074	0.112 ± 0.019	-0.061 ± 0.023
3	0.219 ± 0.023	-0.018 ± 0.015	0.597 ± 0.162	0.358 ± 0.029	0.449 ± 0.025	0.144 ± 0.018
4	0.087 ± 0.041	0.053 ± 0.049	0.027 ± 0.007	-0.003 ± 0.012	0.021 ± 0.006	-0.012 ± 0.018
5	0.017 ± 0.006	0.001 ± 0.013	0.125 ± 0.036	0.023 ± 0.029	0.088 ± 0.041	0.038 ± 0.041
6	0.177 ± 0.027	0.002 ± 0.008	0.335 ± 0.028	-0.211 ± 0.022	0.292 ± 0.027	-0.091 ± 0.016
7	0.431 ± 0.021	0.131 ± 0.016	0.056 ± 0.013	-0.102 ± 0.055	0.130 ± 0.046	-0.074 ± 0.048
8	0.279 ± 0.022	0.063 ± 0.050	0.012 ± 0.132	0.003 ± 0.244	0.039 ± 0.129	0.029 ± 0.243

Table 6. The values of Δc_i and Δs_i parameters under three binning schemes. The differences between the $K^0_S\pi^+\pi^-$ amplitude models measured by the Belle and BESIII experiments and the uncertainties of the U-spin breaking parameters are assigned as the uncertainties.

Bin	Δc_i	Δs_i	Δc_i	Δs_i	Δc_i	Δs_i
	Equal		Optimal		Modified optimal	
1	0.105 ± 0.026	0.028 ± 0.098	0.202 ± 0.053	0.057 ± 0.194	0.156 ± 0.067	0.031 ± 0.228
2	0.114 ± 0.051	0.270 ± 0.202	-0.043 ± 0.088	0.239 ± 0.234	0.079 ± 0.043	0.069 ± 0.142
3	0.251 ± 0.049	0.358 ± 0.197	0.474 ± 0.100	0.224 ± 0.280	0.365 ± 0.048	0.180 ± 0.155
4	0.006 ± 0.064	0.052 ± 0.256	0.057 ± 0.025	-0.069 ± 0.112	0.086 ± 0.027	0.054 ± 0.128
5	0.046 ± 0.028	-0.030 ± 0.130	0.109 ± 0.044	0.020 ± 0.187	-0.011 ± 0.049	-0.042 ± 0.213
6	0.281 ± 0.066	-0.179 ± 0.244	0.377 ± 0.094	0.328 ± 0.294	0.331 ± 0.060	0.191 ± 0.211
7	0.313 ± 0.064	0.085 ± 0.228	0.030 ± 0.027	0.049 ± 0.114	0.023 ± 0.035	0.156 ± 0.131
8	0.136 ± 0.046	0.015 ± 0.162	-0.012 ± 0.041	0.120 ± 0.159	-0.023 ± 0.042	0.060 ± 0.174

Table 7. The Δc_i and Δs_i parameters calculated with the unconstrained strong-phase parameters as listed in table 4 under three binning schemes.

JHEP06(2025)086

C Systematic uncertainties

Uncertainty (10^{-4})	c_1	c_2	c_3	c_4	c_5	c_6	c_7	c_8	s_1	s_2	s_3	s_4	s_5	s_6	s_7	s_8
$K_i^{(\prime)}$ inputs	26	79	27	55	37	97	45	56	37	134	88	98	27	32	102	49
Input parameters	5	18	17	13	3	25	27	19	37	122	18	12	22	32	41	49
ST yields	60	79	75	55	29	63	104	78	16	73	53	73	7	64	61	41
MC statistics	37	43	14	63	34	46	18	37	11	73	97	172	11	107	112	41
Background	17	14	20	50	45	50	27	22	21	61	44	86	27	12	51	32
Reconstruction	21	31	38	27	9	45	66	39	0	10	6	4	6	2	6	19
Total	80	127	93	116	73	144	138	114	60	218	149	229	46	177	176	97
Uncertainty (10^{-4})	c_1'	c_2'	c_3'	c_4'	c_5'	c_6'	c_7'	c_8'	s_1'	s_2'	s_3'	s_4'	s_5'	s_6'	s_7'	s_8'
$K_i^{(\prime)}$ inputs	31	76	40	32	33	38	71	62	52	72	61	60	85	195	256	146
Input parameters	9	13	10	14	9	14	34	25	9	43	30	0	12	22	73	67
ST yields	36	56	37	28	21	38	59	53	17	29	15	40	12	7	74	32
MC statistics	22	30	13	55	46	72	17	22	17	57	91	121	36	109	73	40
Background	70	59	40	37	79	34	38	62	26	143	137	261	36	239	220	106
Reconstruction	3	8	9	4	0	7	10	7	13	43	25	2	0	5	0	3
Total	88	116	70	81	100	97	107	108	64	183	180	297	101	327	361	200

Table 8. Systematic uncertainties for the equal binning scheme without Δc_i and Δs_i constraints.

Uncertainty (10^{-4})	c_1	c_2	c_3	c_4	c_5	c_6	c_7	c_8	s_1	s_2	s_3	s_4	s_5	s_6	s_7	s_8
$K_i^{(\prime)}$ inputs	32	284	109	33	33	128	43	78	71	201	252	26	61	299	36	49
Input parameters	22	33	55	3	15	64	5	10	36	238	118	21	9	94	36	49
ST yields	86	152	172	29	66	121	54	62	90	37	34	27	83	56	65	39
MC statistics	18	40	31	45	24	21	37	34	80	73	67	16	104	187	14	29
Background	18	26	47	39	42	50	24	29	53	73	84	31	52	131	71	87
Reconstruction	49	91	121	13	35	76	16	19	10	17	8	11	6	9	11	7
Total	109	340	250	75	96	209	83	111	154	331	300	57	156	392	110	122
Uncertainty (10^{-4})	c_1'	c_2'	c_3'	c_4'	c_5'	c_6'	c_7'	c_8'	s_1'	s_2'	s_3'	s_4'	s_5'	s_6'	s_7'	s_8'
$K_i^{(\prime)}$ inputs	43	172	198	29	19	189	37	73	140	184	260	50	41	145	52	70
Input parameters	18	59	104	6	9	41	9	14	31	117	12	40	14	83	26	56
ST yields	43	73	83	15	31	68	34	31	15	66	79	98	51	40	17	55
MC statistics	18	25	10	57	25	20	36	30	140	67	80	30	149	207	26	42
Background	25	76	47	68	16	77	80	103	203	50	160	80	122	186	26	181
Reconstruction	8	12	16	2	6	14	0	2	9	28	14	9	4	48	19	1
Total	71	212	244	95	48	220	101	133	286	244	347	145	203	331	74	212

Table 9. Systematic uncertainties for the optimal binning scheme without Δc_i and Δs_i constraints.

JHEP06(2025)086

Uncertainty (10^{-4})	c_1	c_2	c_3	c_4	c_5	c_6	c_7	c_8	s_1	s_2	s_3	s_4	s_5	s_6	s_7	s_8
$K_i^{(\prime)}$ inputs	60	111	41	33	36	53	35	56	51	92	97	23	62	116	36	61
Input parameters	17	9	31	3	13	31	5	8	51	110	81	17	10	46	36	41
ST yields	77	90	112	22	59	92	69	65	51	47	57	30	91	80	36	42
MC statistics	26	39	10	32	26	22	39	34	165	37	41	23	124	70	27	31
Background	56	18	31	35	50	31	32	31	76	74	49	34	93	93	82	71
Reconstruction	42	68	101	2	36	51	26	28	0	7	9	6	0	13	8	13
Total	124	164	162	61	97	127	96	102	202	172	152	59	190	189	107	117
Uncertainty (10^{-4})	c_1'	c_2'	c_3'	c_4'	c_5'	c_6'	c_7'	c_8'	s_1'	s_2'	s_3'	s_4'	s_5'	s_6'	s_7'	s_8'
$K_i^{(\prime)}$ inputs	20	76	64	32	18	119	43	64	97	109	167	48	31	79	46	58
Input parameters	10	28	42	8	11	25	7	12	77	69	71	36	16	47	35	44
ST yields	39	48	56	19	24	47	41	32	56	20	46	11	60	46	11	72
MC statistics	20	16	8	40	32	54	24	26	193	40	24	48	62	79	23	44
Background	29	76	31	80	14	58	77	99	251	50	107	95	172	221	93	175
Reconstruction	7	6	11	0	4	11	4	4	4	24	5	7	9	44	21	6
Total	58	122	101	97	47	153	101	125	345	147	217	122	195	260	114	208

Table 10. Systematic uncertainties for the modified optimal binning scheme without Δc_i and Δs_i constraints.

Uncertainty (10^{-4})	c_1	c_2	c_3	c_4	c_5	c_6	c_7	c_8	s_1	s_2	s_3	s_4	s_5	s_6	s_7	s_8
$K_i^{(\prime)}$ inputs	21	50	23	31	21	54	48	43	25	49	25	38	15	31	71	27
Input parameters	5	11	8	7	5	7	29	19	30	41	0	10	15	20	27	21
ST yields	56	67	55	44	17	44	70	60	4	17	39	39	10	54	61	42
MC statistics	32	34	5	51	39	44	10	26	10	42	62	94	25	107	41	18
Background	27	25	18	44	52	40	16	24	15	49	64	97	15	104	72	35
Reconstruction	22	30	37	25	10	44	62	38	0	13	5	0	6	4	6	21
Total	76	99	70	89	71	102	111	92	44	94	101	108	37	163	128	68
Uncertainty (10^{-4})	c_1'	c_2'	c_3'	c_4'	c_5'	c_6'	c_7'	c_8'	s_1'	s_2'	s_3'	s_4'	s_5'	s_6'	s_7'	s_8'
$K_i^{(\prime)}$ inputs	26	57	29	25	21	49	54	48	25	42	25	30	15	31	71	37
input parameters	8	10	5	7	6	3	31	18	6	34	0	10	15	21	27	14
ST yields	36	57	47	37	15	39	64	50	18	17	39	30	11	54	52	38
MC statistics	21	30	5	47	38	49	10	22	16	44	64	94	24	102	40	12
Background	55	42	18	35	56	37	22	41	12	59	64	101	15	104	72	35
Reconstruction	3	7	8	3	0	6	11	6	13	32	19	0	3	2	3	3
Total	74	97	60	74	73	88	93	85	39	98	104	145	38	160	123	66

Table 11. Systematic uncertainties for the equal binning scheme with Δc_i and Δs_i constraints.

JHEP06(2025)086

D Correlation matrices of statistical and systematic uncertainties

Uncertainty (10^{-4})	c_1	c_2	c_3	c_4	c_5	c_6	c_7	c_8	s_1	s_2	s_3	s_4	s_5	s_6	s_7	s_8
$K_i^{(\prime)}$ inputs	25	148	94	21	21	121	30	72	65	106	132	17	43	274	24	31
Input parameters	14	39	49	5	8	13	4	8	22	54	12	19	5	36	23	19
ST yields	64	83	170	17	55	81	48	65	56	14	48	19	42	50	23	28
MC statistics	14	18	21	35	21	14	26	33	67	58	77	20	55	108	15	30
Background	11	60	42	50	31	35	45	31	86	54	94	33	45	83	41	103
Reconstruction	48	93	118	15	34	73	15	17	3	2	14	9	3	19	15	12
Total	87	207	236	69	72	167	78	109	140	144	186	51	92	313	59	116
Uncertainty (10^{-4})	c_1'	c_2'	c_3'	c_4'	c_5'	c_6'	c_7'	c_8'	s_1'	s_2'	s_3'	s_4'	s_5'	s_6'	s_7'	s_8'
$K_i^{(\prime)}$ inputs	30	148	158	22	16	127	31	72	65	107	133	18	43	278	24	61
input parameters	14	41	96	5	3	16	7	13	22	26	12	15	5	36	12	36
ST yields	53	83	75	16	34	77	38	30	57	26	60	19	39	50	12	60
MC statistics	14	17	14	37	21	15	21	20	66	62	77	20	54	107	18	36
Background	14	61	43	55	18	45	56	96	86	52	95	34	47	83	30	155
Reconstruction	9	12	16	0	6	14	2	3	9	26	17	7	5	29	18	0
Total	66	186	205	72	47	158	78	126	139	142	192	50	92	316	49	184

Table 12. Systematic uncertainties for the optimal binning scheme with Δc_i and Δs_i constraints.

Uncertainty (10^{-4})	c_1	c_2	c_3	c_4	c_5	c_6	c_7	c_8	s_1	s_2	s_3	s_4	s_5	s_6	s_7	s_8
$K_i^{(\prime)}$ inputs	57	67	34	23	27	60	29	53	30	51	77	31	41	91	60	36
Input parameters	12	10	25	5	8	9	4	7	20	20	32	29	13	8	70	19
ST yields	78	63	80	14	57	81	46	65	33	13	50	27	40	54	15	47
MC statistics	33	24	5	33	30	12	35	30	84	27	43	41	62	71	20	25
Background	53	42	13	52	39	19	34	29	90	27	52	46	54	108	70	106
Reconstruction	42	67	103	5	36	51	26	27	0	2	4	11	3	13	6	8
Total	123	124	138	68	88	116	78	98	132	68	118	80	101	168	119	126
Uncertainty (10^{-4})	c_1'	c_2'	c_3'	c_4'	c_5'	c_6'	c_7'	c_8'	s_1'	s_2'	s_3'	s_4'	s_5'	s_6'	s_7'	s_8'
$K_i^{(\prime)}$ inputs	19	63	46	23	17	75	37	63	31	52	78	31	40	90	60	53
Input parameters	4	18	32	5	6	12	8	11	20	13	33	30	7	8	45	38
ST yields	41	53	62	17	26	57	44	31	22	13	57	22	35	78	14	74
MC statistics	21	20	4	33	24	13	22	23	86	28	42	47	60	70	21	29
Background	22	55	16	53	20	32	67	89	103	27	53	42	56	108	45	152
Reconstruction	7	5	11	0	4	10	4	3	4	20	4	11	8	26	19	1
Total	55	103	86	69	45	102	91	116	141	70	123	80	98	177	93	184

Table 13. Systematic uncertainties for the modified optimal binning scheme with Δc_i and Δs_i constraints.

JHEP06(2025)086

	c_2	c_3	c_4	c_5	c_6	c_7	c_8	s_1	s_2	s_3	s_4	s_5	s_6	s_7	s_8	c'_1	c'_2	c'_3	c'_4	c'_5	c'_6	c'_7	c'_8	s'_1	s'_2	s'_3	s'_4	s'_5	s'_6	s'_7	s'_8
c_1	−11	−1	0	0	−1	0	−15	0	0	0	0	0	0	0	0	−1	0	0	3	3	0	0	0	0	0	0	0	0	0	0	0
c_2		−7	0	0	0	−2	−1	0	−1	0	0	0	1	0	−1	1	0	0	0	2	2	−1	−1	−1	0	0	0	3	1	0	0
c_3			−6	−1	−1	−1	−2	0	0	2	1	1	0	0	−2	0	−1	0	1	0	0	−1	0	−1	−1	0	−1	3	2	−1	−2
c_4				−6	−2	−1	1	−1	0	−1	2	0	1	1	0	1	2	1	0	−1	0	0	2	−1	1	1	−1	0	0	−1	−3
c_5					−10	0	0	0	0	0	0	−5	1	0	0	5	3	0	0	−1	0	0	3	0	0	0	0	0	0	0	0
c_6						−9	0	0	1	0	0	−1	−5	1	1	−1	2	1	0	−1	0	0	1	2	2	0	0	0	−1	0	1
c_7							−13	2	0	0	0	0	0	−1	4	0	0	1	0	0	−1	−1	0	4	6	3	−3	−2	−1	1	2
c_8								1	0	0	0	−1	0	1	1	0	0	0	0	1	0	0	−1	1	1	1	−1	−3	−1	1	1
s_1									8	11	−6	0	0	−4	−10	0	−1	−3	−2	1	2	3	0	8	−6	−1	−2	21	6	12	−5
s_2										2	3	6	−11	−1	0	0	0	−1	−2	1	4	1	0	20	−12	−18	0	30	36	−3	−9
s_3											−2	−1	−3	−8	−16	0	0	0	0	0	0	1	0	1	−9	−25	−16	7	16	20	10
s_4												−3	−7	−8	−8	0	0	−1	−1	0	−1	−1	−1	−2	−18	−23	−16	−1	9	17	25
s_5													−13	5	−3	0	2	2	−1	0	−1	0	−1	8	7	−1	−6	6	4	−8	−5
s_6														−4	1	0	1	4	1	0	−1	−1	0	1	9	25	5	−3	−1	−8	−4
s_7															−10	0	−1	0	0	0	0	0	0	7	24	28	22	−4	−7	−16	−6
s_8																0	−1	−4	−1	0	1	1	0	2	5	24	15	−4	−8	−8	−6
c'_2																	−14	1	−1	−1	−1	3	−25	−1	0	0	0	0	0	0	0
c'_3																		−8	0	−1	−1	0	2	0	−2	0	0	0	0	0	0
c'_4																			−7	0	−1	0	0	0	1	0	−1	−1	0	−1	0
c'_5																				−5	0	0	0	−1	0	0	2	−1	−1	0	0
c'_6																					−10	0	−1	0	0	0	0	0	1	0	0
c'_7																						−16	2	1	0	0	0	2	−1	0	−1
c'_8																							−24	0	0	0	0	1	1	2	−1
c'_9																								0	0	0	0	0	0	0	1
s'_1																									−10	0	1	7	7	−1	−19
s'_2																										11	9	−5	−8	−10	−5
s'_3																											12	−8	−14	−14	−9
s'_4																												−5	−6	−9	−7
s'_5																													6	3	−3
s'_6																														−7	1
s'_7																															−10

Table 14. Correlation matrix (%) of statistical uncertainties for the equal binning scheme without Δc_i and Δs_i constraints.

JHEP06(2025)086

	c_2	c_3	c_4	c_5	c_6	c_7	c_8	s_1	s_2	s_3	s_4	s_5	s_6	s_7	s_8	c'_1	c'_2	c'_3	c'_4	c'_5	c'_6	c'_7	c'_8	s'_1	s'_2	s'_3	s'_4	s'_5	s'_6	s'_7	s'_8
c_1	−2	−7	−3	−1	−1	−2	−2	−3	3	1	−2	−1	0	2	−1	−1	−1	0	1	−1	1	0	1	1	3	3	−2	−1	6	4	−3
c_2		−13	0	0	−8	−4	0	0	−3	1	0	0	0	0	0	1	0	−2	2	1	−1	1	1	0	0	0	−1	0	0	0	0
c_3			0	−1	−3	−1	−1	1	6	−4	−2	−1	1	0	−2	0	−2	−1	−1	−1	0	0	1	1	3	2	0	0	3	1	−2
c_4				−3	0	0	−1	1	0	0	−5	0	0	0	0	1	3	1	−1	0	1	7	3	0	0	1	0	0	0	1	−1
c_5					−5	−1	0	0	−1	0	−1	2	0	1	2	0	0	0	−1	1	−1	1	0	−1	−1	−1	4	−3	0	1	2
c_6						0	0	0	−3	0	1	1	−2	0	1	0	1	−1	0	2	−2	0	1	−1	−3	−2	2	0	0	−1	1
c_7							0	1	0	0	0	0	0	−5	0	0	−1	−1	7	−1	0	−1	0	−1	0	−1	1	1	0	0	0
c_8								0	0	0	0	0	0	0	3	−1	0	0	3	−1	−1	−1	0	−1	0	0	1	0	0	0	1
s_1									−8	−7	−4	−6	−5	−17	4	0	0	0	−1	−1	0	0	0	−18	−1	1	−7	19	36	15	−10
s_2										−16	−5	−5	−4	6	−7	2	−1	1	1	−3	−2	0	0	12	14	−1	10	6	1	−4	−2
s_3											−1	−5	−9	2	5	0	0	0	0	−1	−1	0	0	−8	−2	−12	−6	8	8	2	−2
s_4												0	1	−3	5	−2	0	0	0	3	1	1	0	1	6	−10	0	10	−7	4	12
s_5													−6	12	3	−1	0	0	0	0	0	0	0	23	−6	10	16	−49	−12	−10	2
s_6														8	1	1	0	0	0	0	0	0	0	14	0	7	15	−1	−12	5	5
s_7															−1	2	0	1	3	−1	−2	0	0	17	−13	7	26	−14	−15	−1	3
s_8																−2	0	0	−1	0	0	0	0	−12	3	2	−4	3	9	0	13
c'_2																	−2	−15	−6	−1	−1	−2	−3	−1	0	0	1	0	0	0	0
c'_3																		−21	−1	0	−7	−11	0	0	−2	0	0	0	0	0	0
c'_4																			−1	0	0	2	0	0	0	−1	0	0	0	0	0
c'_5																				−2	−1	−1	−1	1	0	0	−2	0	0	0	0
c'_6																					−5	−1	0	0	0	0	0	−4	0	0	1
c'_7																						1	0	0	0	0	−1	0	1	0	0
c'_8																							−3	0	0	0	0	0	0	−3	0
c'_9																								0	0	0	0	0	0	0	1
s'_1																									−4	−7	7	−15	−13	−5	−1
s'_2																										−18	−3	5	−4	−8	0
s'_3																											4	−7	−2	0	−1
s'_4																												−12	−8	−2	1
s'_5																													11	7	−1
s'_6																														6	−4
s'_7																															−4

Table 15. Correlation matrix (%) of statistical uncertainties for the optimal binning scheme without Δc_i and Δs_i constraints.

JHEP06(2025)086

	c_2	c_3	c_4	c_5	c_6	c_7	c_8	s_1	s_2	s_3	s_4	s_5	s_6	s_7	s_8	c'_1	c'_2	c'_3	c'_4	c'_5	c'_6	c'_7	c'_8	s'_1	s'_2	s'_3	s'_4	s'_5	s'_6	s'_7	s'_8
c_1	−1	−3	−4	−1	0	−3	0	−1	0	0	0	0	0	0	0	0	0	0	−1	0	0	0	0	0	0	0	−1	0	1	0	0
c_2		−7	1	−1	−2	−1	−1	0	−2	0	0	0	0	0	0	2	−1	−1	3	2	−1	0	1	0	0	0	−1	0	0	0	0
c_3			−1	−1	−3	−5	−2	−3	7	−1	−1	−2	1	1	−3	0	−1	0	−1	−1	−1	1	1	0	7	4	−2	−2	5	4	−4
c_4				−3	0	0	0	0	1	0	−7	−1	0	0	0	0	3	2	−1	0	1	4	3	0	1	1	0	0	0	0	−1
c_5					−4	0	0	0	−1	1	−1	5	0	0	0	0	3	1	−1	0	1	2	1	1	−1	−1	−1	−4	1	2	0
c_6						−5	0	2	−3	−1	0	1	−3	−1	1	1	0	0	0	1	−1	−1	0	0	−5	−4	5	0	0	−2	3
c_7							2	0	0	0	0	0	0	−2	0	0	−1	−1	6	0	0	0	−1	0	0	0	1	0	0	−1	0
c_8								0	−1	0	0	0	0	0	4	−1	0	0	5	1	0	0	0	0	−1	−1	2	0	0	−1	0
s_1									−3	−19	−8	−2	−1	−6	−4	0	0	0	0	1	1	1	0	1	−12	−7	9	2	1	−15	14
s_2										−7	−5	−4	7	11	−2	1	0	3	1	−2	−4	0	0	17	−2	10	9	−1	5	1	−8
s_3											3	−13	−3	6	8	0	0	0	0	−1	−2	−1	0	3	7	−14	−1	23	24	26	−9
s_4												5	2	2	2	−1	0	−1	0	0	3	1	0	6	7	−8	1	0	−1	12	5
s_5													4	−2	−6	−1	0	−1	0	−1	0	1	0	12	−6	21	−2	−38	−40	−17	15
s_6														5	−5	0	0	1	0	0	0	−1	0	13	7	19	19	−15	−19	8	−5
s_7															6	1	0	2	0	−3	−1	−2	0	12	−6	3	28	4	−7	20	3
s_8																0	0	−1	0	−2	3	1	0	−9	−5	−9	−6	16	6	5	−1
c'_2																	0	−2	−4	−1	0	−5	−1	−1	0	0	1	0	0	0	0
c'_3																		−13	−1	−1	−1	−3	−2	0	−3	0	0	0	0	0	0
c'_4																			−3	−1	−1	−3	−2	1	0	0	1	0	0	1	0
c'_5																				−1	−1	−1	−1	0	0	0	−3	0	0	0	0
c'_6																					−6	0	0	−1	0	0	−1	−2	0	−1	0
c'_7																						−6	1	−1	0	−1	0	0	−4	0	1
c'_8																							−1	0	0	0	−1	0	0	−5	0
c'_9																								0	0	0	0	0	0	0	1
s'_1																									0	4	4	−7	−6	−1	0
s'_2																										−10	−2	1	1	1	−6
s'_3																											2	−14	−15	−6	−1
s'_4																												−3	−5	5	1
s'_5																													18	10	−5
s'_6																														6	−7
s'_7																															−6

Table 16. Correlation matrix (%) of statistical uncertainties for the modified optimal binning scheme without Δc_i and Δs_i constraints.

	c_2	c_3	c_4	c_5	c_6	c_7	c_8	s_1	s_2	s_3	s_4	s_5	s_6	s_7	s_8	c'_1	c'_2	c'_3	c'_4	c'_5	c'_6	c'_7	c'_8	s'_1	s'_2	s'_3	s'_4	s'_5	s'_6	s'_7	s'_8
c_1	72	73	33	0	27	68	74	25	22	37	10	6	−19	−29	−28	49	43	38	−21	−23	−20	30	46	0	23	28	16	1	−1	−15	−12
c_2		64	32	3	26	62	61	11	28	27	11	1	−18	−26	−28	30	29	25	−11	−10	−11	20	31	5	19	19	8	10	11	−6	−3
c_3			59	31	54	89	77	18	18	13	14	−11	−22	−13	−14	13	20	14	17	21	11	18	18	−1	6	5	−20	−3	14	−4	0
c_4				55	53	57	48	11	4	−30	−42	−9	28	34	2	0	0	−12	29	33	13	0	−1	−10	−25	−21	−39	−5	29	2	3
c_5					42	32	20	3	−10	−39	−22	−31	27	36	10	−27	−21	−30	33	45	19	−15	−25	5	−27	−28	−42	0	33	23	27
c_6						55	40	3	−3	−19	−4	−13	12	15	−2	−13	−8	−11	27	32	15	−3	−9	8	−3	−15	−34	0	27	20	25
c_7							75	15	16	12	12	−9	−17	−6	−3	11	18	13	16	18	11	16	15	5	13	9	−16	−4	10	−6	0
c_8								25	24	20	7	−2	−11	−8	−14	24	27	19	−1	5	−5	17	25	−1	4	14	−7	−4	11	−10	−5
s_1									46	28	18	10	−9	1	6	2	22	17	1	22	19	1	6	15	−28	−16	−19	39	26	4	−8
s_2										36	21	19	−18	−10	2	9	24	29	−1	11	20	13	15	18	−9	−19	−11	37	24	−16	−17
s_3											56	2	−51	−52	−33	25	33	45	−27	−19	−2	19	30	26	19	8	14	33	8	11	3
s_4												−24	−72	−53	−19	−3	23	21	17	17	31	16	5	15	−4	−12	−17	17	12	28	21
s_5													28	13	23	19	12	26	−33	−33	−22	4	14	10	18	18	37	5	−15	−32	−36
s_6														60	22	−10	−20	−27	−24	−12	−38	−33	−22	9	−9	0	10	0	21	8	9
s_7															32	−25	−31	−25	13	19	3	−28	−34	5	−13	−17	−17	5	16	5	11
s_8																−19	−14	−11	6	3	16	−19	−21	8	5	10	10	0	−16	−20	−26
c'_2																	57	61	−24	−57	−14	47	66	−21	28	40	39	−10	−28	−31	−26
c'_3																		52	−6	−24	6	43	55	2	−6	23	25	5	−8	−14	−18
c'_4																			−3	−30	11	54	62	4	31	35	39	1	−31	−33	−32
c'_5																				68	72	14	−12	−21	−36	−32	−46	−11	10	8	10
c'_6																					60	−9	−36	−6	−53	−47	−65	21	36	27	24
c'_7																						27	1	−9	−28	−22	−37	0	13	−3	−6
c'_8																							44	−18	15	20	16	−14	−26	−51	−22
c'_9																								−7	22	33	33	−6	−25	−26	−45
s'_1																									19	−6	8	47	33	33	26
s'_2																										56	58	−9	−45	−28	−13
s'_3																											70	−28	−55	−35	−28
s'_4																												−12	−54	−38	−35
s'_5																													47	33	23
s'_6																														60	52
s'_7																															66

Table 17. Correlation matrix (%) of systematic uncertainties for the equal binning scheme without Δc_i and Δs_i constraints.

	c_2	c_3	c_4	c_5	c_6	c_7	c_8	s_1	s_2	s_3	s_4	s_5	s_6	s_7	s_8	c'_1	c'_2	c'_3	c'_4	c'_5	c'_6	c'_7	c'_8	s'_1	s'_2	s'_3	s'_4	s'_5	s'_6	s'_7	s'_8
c_1	50	85	38	84	70	49	32	−10	5	−3	5	22	2	30	2	27	11	14	23	29	11	2	0	8	−1	−5	16	−23	8	8	−8
c_2		46	8	43	42	39	25	−17	10	−3	0	21	6	14	−7	13	14	9	−3	7	12	14	11	−6	4	−6	6	−4	12	10	−14
c_3			32	79	68	46	30	−12	11	−19	9	21	4	30	1	21	11	12	20	20	12	−1	−1	6	−3	−8	16	−20	7	9	−5
c_4				54	23	−26	−17	30	−10	5	9	−22	−15	23	42	3	−19	−3	74	38	−14	−54	−46	57	−4	30	37	−44	−19	5	43
c_5					66	37	23	−2	6	2	14	2	−5	44	18	20	2	10	44	33	3	−18	−16	26	−11	1	29	−41	−7	3	20
c_6						47	31	−22	−2	−12	3	25	38	29	3	17	12	12	12	14	9	4	−2	5	6	1	22	−13	12	14	−7
c_7							51	−44	6	−13	−2	42	12	20	−18	27	32	22	−30	7	25	47	35	−25	3	−18	9	8	23	6	−33
c_8								−32	1	−10	−2	33	7	12	−16	17	19	12	−22	3	22	33	26	−15	9	−4	11	11	24	11	−23
s_1									5	25	23	−61	−29	−6	25	−20	−22	−15	28	−2	−18	−30	−24	42	3	30	8	−39	−34	3	39
s_2										24	22	0	14	26	−31	−1	3	−2	−1	−1	10	6	4	−15	−28	−36	−21	−5	−20	−24	7
s_3											28	−19	−3	17	−9	−10	−5	−11	10	−5	5	−9	−10	5	−24	−10	−6	−17	−27	−22	26
s_4												−8	4	37	10	−10	−9	−5	22	2	−6	−15	−23	21	−27	−7	27	−11	−31	−20	53
s_5													37	21	−23	18	18	12	−15	7	24	24	21	−31	−3	−15	4	36	57	−7	−34
s_6														13	−38	3	8	2	−11	0	10	13	3	−30	−12	−31	−14	41	20	−12	−16
s_7															5	14	0	8	46	30	7	−19	−26	33	−28	−7	37	−34	−25	−13	39
s_8																−20	−21	−8	37	2	−18	−38	−30	53	14	56	45	−41	−2	16	52
c'_2																	32	27	6	62	29	34	33	−29	−13	−24	−16	−3	6	−16	−29
c'_3																		18	−23	22	20	40	37	−23	−13	−17	−16	9	11	−2	−30
c'_4																			−3	29	20	23	19	−5	−2	−38	−5	2	8	−1	−16
c'_5																				45	−14	−69	−58	60	−18	22	40	−48	−27	−12	52
c'_6																					22	3	5	16	−17	−8	2	−21	−3	−17	−3
c'_7																						31	31	−18	−2	−13	−13	5	33	−5	−24
c'_8																							71	−51	6	−28	−34	31	25	−7	−50
c'_9																								−48	4	−20	−39	22	35	−4	−49
s'_1																									23	63	65	−57	−33	27	53
s'_2																										52	24	18	28	65	−26
s'_3																											57	−26	14	49	23
s'_4																												−23	−6	31	43
s'_5																													49	19	−43
s'_6																														22	−42
s'_7																															−15

Table 18. Correlation matrix (%) of systematic uncertainties for the optimal binning scheme without Δc_i and Δs_i constraints.

	c_2	c_3	c_4	c_5	c_6	c_7	c_8	s_1	s_2	s_3	s_4	s_5	s_6	s_7	s_8	c'_1	c'_2	c'_3	c'_4	c'_5	c'_6	c'_7	c'_8	s'_1	s'_2	s'_3	s'_4	s'_5	s'_6	s'_7	s'_8
c_1	44	73	47	76	66	36	36	11	21	−11	−10	20	−3	29	7	17	−6	11	43	28	−11	−10	−20	39	−2	18	34	−51	−18	−14	16
c_2		63	2	46	60	60	55	−11	12	−20	−17	21	21	15	−9	20	20	20	−3	−2	16	23	16	11	8	−6	7	−8	22	14	−17
c_3			26	76	82	59	57	−8	20	−12	−19	26	16	24	−2	23	10	18	22	19	7	7	−1	19	5	0	15	−29	10	7	−4
c_4				53	21	−21	−12	23	13	9	5	−7	−31	16	23	2	−30	−11	58	36	−34	−43	−46	45	−6	34	41	−57	−47	−32	38
c_5					69	37	36	12	27	−5	1	5	−6	32	10	18	−7	11	46	29	−16	−12	−21	44	−21	7	39	−57	−29	−24	29
c_6						64	59	−11	11	−28	−25	26	26	21	−5	18	12	18	16	8	6	10	1	26	8	6	22	−27	14	10	−12
c_7							72	−12	3	−35	−28	23	33	11	−22	32	43	36	−25	−9	29	51	39	9	5	−21	2	4	41	25	−40
c_8								−22	6	−28	−28	31	30	13	−12	26	32	26	−16	−7	27	38	29	3	11	−8	5	−2	30	17	−26
s_1									−7	17	45	−60	−31	−15	11	−18	−16	−18	−1	−16	−19	−12	−8	40	−24	−1	31	−4	−13	−20	18
s_2										21	7	28	17	52	−24	20	−6	6	39	17	13	−10	−17	12	−31	−10	2	−37	−28	−29	23
s_3											37	−20	−11	10	−2	−10	−19	−23	9	−4	6	−21	−14	−9	−15	−5	−7	4	−14	−12	23
s_4												−40	−27	9	23	−32	−25	−26	5	−26	−16	−23	−19	27	−30	1	31	−5	−34	−27	47
s_5													42	37	−14	25	10	19	28	23	26	10	0	−14	5	17	−4	−37	−12	−10	6
s_6														21	−33	30	27	21	−12	0	43	34	27	−21	8	−8	−17	13	30	26	−36
s_7															−13	17	−9	10	45	17	9	−15	−27	35	−21	8	34	−46	−34	−17	28
s_8																−26	−20	−19	11	−2	−36	−19	−14	8	2	27	30	−9	−36	−15	38
c'_2																	46	58	11	63	31	46	32	2	−4	−20	−19	−15	14	7	−25
c'_3																		41	−40	8	36	65	58	−20	−4	−26	−26	22	36	24	−39
c'_4																			−5	34	34	45	35	−2	0	−34	−13	−3	18	14	−24
c'_5																				54	−28	−54	−60	42	−21	33	39	−71	−62	−49	54
c'_6																					6	−3	−10	7	−10	3	−4	−39	−23	−13	9
c'_7																						41	39	−24	13	−19	−27	26	45	27	−33
c'_8																							73	−27	4	−33	−30	33	43	24	−45
c'_9																								−39	9	−34	−36	48	49	36	−44
s'_1																									−8	39	69	−57	−28	−29	23
s'_2																										40	1	27	45	51	−37
s'_3																											55	−31	−21	−10	26
s'_4																												−49	−44	−27	44
s'_5																													70	58	−55
s'_6																														69	−80
s'_7																															−65

Table 19. Correlation matrix (%) of systematic uncertainties for the modified optimal binning scheme without Δc_i and Δs_i constraints.

	c_2	c_3	c_4	c_5	c_6	c_7	c_8	s_1	s_2	s_3	s_4	s_5	s_6	s_7	s_8	c'_1	c'_2	c'_3	c'_4	c'_5	c'_6	c'_7	c'_8	s'_1	s'_2	s'_3	s'_4	s'_5	s'_6	s'_7	s'_8
c_1	−9	−1	1	3	−1	1	−14	−1	0	0	0	0	0	0	0	34	−7	0	2	3	−1	1	−13	−1	0	0	0	0	0	0	0
c_2		−7	1	2	1	−1	0	−1	−2	0	0	2	1	−1	−1	−8	56	−6	0	1	2	−1	0	−1	−2	0	0	3	1	−1	−1
c_3			−4	0	−1	−1	−1	−2	−2	1	0	1	2	−1	−3	0	−6	69	−4	0	−1	−1	−1	−2	−2	1	0	1	2	−1	−3
c_4				−5	−2	−1	1	−2	−1	0	0	0	1	−1	−2	1	1	−4	53	−5	−1	0	2	−2	−1	0	0	0	1	−1	−3
c_5					−10	0	2	0	0	0	0	−3	0	0	0	3	2	0	−5	91	−9	0	2	0	0	0	0	0	−3	0	0	0
c_6						−11	1	1	2	0	0	−1	−4	1	2	−1	1	0	−1	−9	74	−11	1	2	2	0	0	−1	−4	1	2
c_7							−15	4	3	1	−1	−1	−2	0	3	2	0	0	−1	0	−12	81	−17	4	3	1	−1	−1	−2	0	3
c_8								1	1	1	−1	−2	−1	1	1	−15	0	−1	0	2	1	−16	67	1	1	1	−1	−2	−1	1	1
s_1									2	7	−8	10	3	7	−10	−1	−1	−2	−2	0	1	4	1	40	1	7	−8	10	3	7	−10
s_2										−14	−2	13	10	9	0	0	−2	−1	−1	0	2	3	0	5	87	−14	−2	13	10	9	−2
s_3											−19	−1	12	8	3	0	0	1	0	0	0	1	0	4	−13	97	−18	−1	12	8	3
s_4												−7	0	14	11	0	0	0	0	0	0	−1	−1	−1	−2	−18	88	−7	0	14	13
s_5													−10	1	−5	0	2	1	−1	−3	−1	0	−1	8	12	−1	−7	97	−10	1	−5
s_6														−19	−7	0	1	2	1	0	−4	−1	−1	3	8	12	0	−9	100	−19	−5
s_7															−23	0	0	−1	0	0	1	0	0	8	9	8	14	1	−19	98	−20
s_8																0	−1	−3	−2	0	1	3	1	−9	0	3	11	−5	−7	−23	79
c'_2																	−11	0	1	3	−1	2	−20	−1	0	0	0	0	0	0	0
c'_3																		−7	0	2	1	−1	0	−1	−2	0	0	2	1	0	−1
c'_4																			−5	0	0	0	−1	−1	−1	1	0	1	2	−1	−3
c'_5																				−5	−1	−1	1	−1	−1	0	0	−1	1	0	−2
c'_6																					−9	0	2	0	0	0	0	−3	0	0	0
c'_7																						−13	1	1	2	0	0	−1	−4	1	1
c'_8																							−19	3	3	1	−1	0	−1	0	3
c'_9																								1	0	0	−1	−1	−1	0	1
s'_1																									3	4	−1	8	3	8	−11
s'_2																										−13	−2	12	8	9	−2
s'_3																											−17	−1	12	8	4
s'_4																												−7	0	14	12
s'_5																													−9	1	−5
s'_6																														−19	−5
s'_7																															−20

Table 20. Correlation matrix (%) of statistical uncertainties for the equal binning scheme with Δc_i and Δs_i constraints.

	c_2	c_3	c_4	c_5	c_6	c_7	c_8	s_1	s_2	s_3	s_4	s_5	s_6	s_7	s_8	c'_1	c'_2	c'_3	c'_4	c'_5	c'_6	c'_7	c'_8	s'_1	s'_2	s'_3	s'_4	s'_5	s'_6	s'_7	s'_8
c_1	−2	−6	−3	−1	−1	−1	−2	−2	4	2	−3	−2	2	4	−2	68	−2	−8	−3	−1	−1	−1	−1	−2	4	2	−3	−2	2	4	−3
c_2		−10	2	0	−6	−7	0	0	−3	1	0	0	0	0	0	−2	96	−18	2	0	−7	−8	1	0	−3	1	0	0	0	0	0
c_3			−1	−1	−2	0	−1	1	5	0	−1	−1	2	1	−2	−5	−10	14	−1	−1	−2	0	1	1	5	0	−1	−1	2	1	−2
c_4				−3	0	6	1	0	1	0	−5	−1	0	2	−1	−3	2	0	85	−2	0	6	2	0	1	0	−5	−1	0	1	−1
c_5					−4	−1	0	−1	−2	−1	1	−1	−1	−1	2	−1	1	0	−3	43	−4	0	0	−1	−2	−1	1	−1	−1	−1	2
c_6						0	0	−1	−4	−2	2	1	−1	−2	1	−1	−6	0	0	−3	82	0	1	−1	−4	−2	2	1	−1	−2	1
c_7							0	0	0	−1	2	0	0	−4	1	−1	−7	0	6	−1	0	65	−1	0	0	−1	2	0	0	−3	0
c_8								0	0	0	1	0	0	−1	3	−1	0	0	1	0	0	0	4	0	0	0	1	0	0	0	1
s_1									−1	−12	−1	17	13	4	−5	−2	0	0	0	−1	0	0	0	98	−2	−12	−1	17	13	6	−9
s_2										−16	2	−1	−5	−7	−2	3	−3	1	1	−2	−3	0	0	−1	86	−16	2	−1	−5	−8	−2
s_3											−7	3	1	8	4	2	1	−1	0	−1	−1	0	0	−12	−16	97	−7	3	1	5	−1
s_4												11	0	9	5	−3	0	0	−4	2	2	1	0	−1	2	−7	97	10	−1	6	10
s_5													−10	−4	5	−2	0	0	−1	−2	1	0	0	17	−1	3	11	86	−10	−2	1
s_6														−1	7	2	0	0	0	0	−1	0	0	13	−4	1	0	−10	99	1	3
s_7															3	3	0	0	2	0	−1	−3	0	4	−9	8	9	−4	−2	66	2
s_8																−2	0	0	−1	1	1	0	1	−5	−1	4	5	5	7	1	29
c'_2																	−2	−12	−4	−1	−1	−2	−2	−2	3	2	−2	−2	2	3	−2
c'_3																		−19	2	0	−7	−9	1	0	−3	1	0	0	0	0	0
c'_4																			0	0	0	1	0	0	1	−1	0	0	0	0	0
c'_5																				−2	0	5	2	0	0	0	−4	−1	0	1	−1
c'_6																					−4	−1	0	−1	−2	−1	2	−2	0	0	1
c'_7																						0	1	0	−3	−1	2	1	−1	−1	1
c'_8																							−2	0	0	0	1	0	0	−3	0
c'_9																								0	0	0	0	0	0	0	1
s'_1																									−1	−12	−1	16	13	6	−9
s'_2																										−16	2	0	−4	−10	−1
s'_3																											−7	3	1	5	−1
s'_4																												10	0	6	9
s'_5																													−9	−2	1
s'_6																														1	3
s'_7																															0

Table 21. Correlation matrix (%) of statistical uncertainties for the optimal binning scheme with Δc_i and Δs_i constraints.

	c_2	c_3	c_4	c_5	c_6	c_7	c_8	s_1	s_2	s_3	s_4	s_5	s_6	s_7	s_8	c'_1	c'_2	c'_3	c'_4	c'_5	c'_6	c'_7	c'_8	s'_1	s'_2	s'_3	s'_4	s'_5	s'_6	s'_7	s'_8
c_1	0	−2	−3	−1	0	−3	0	−1	1	0	0	0	0	0	0	17	0	−2	−3	−1	0	−1	0	−1	1	0	0	0	0	0	0
c_2		−8	3	1	−1	−1	−1	0	−3	0	0	0	0	0	0	1	66	−9	3	1	−1	−2	−1	0	−2	0	0	0	0	0	0
c_3			−1	−1	−2	−4	−1	−2	7	1	−2	−2	3	3	−2	−1	−9	61	−2	−1	−2	−2	0	−2	7	1	−2	−2	3	3	−3
c_4				−3	0	4	3	0	1	1	−4	0	0	1	−1	−3	3	−1	90	−2	1	4	2	0	1	1	−4	0	0	1	−1
c_5					−3	0	1	1	−2	−1	−1	−1	0	−1	0	−1	2	0	−2	41	−2	2	1	1	−2	−1	−1	−1	0	−1	0
c_6						−4	0	2	−6	−3	3	1	−4	−2	2	1	−1	−1	0	−3	68	−4	1	1	−6	−3	3	1	−4	−2	3
c_7							1	0	0	−1	1	0	0	−3	0	−1	−1	−3	4	0	−4	21	−1	0	0	−1	2	0	0	−3	0
c_8								0	−1	0	1	0	0	0	4	−1	−1	−1	4	1	0	0	5	0	−1	0	1	0	0	0	1
s_1									−2	−14	2	0	2	−7	−5	−2	0	−1	0	1	1	0	0	96	−3	−14	3	0	2	−9	9
s_2										−2	2	−5	9	0	−6	1	−3	6	1	−1	−5	0	0	−2	94	−2	2	−5	9	−1	−8
s_3											−4	16	10	13	1	0	0	0	1	−1	−2	0	0	−13	−2	96	−4	16	10	14	−4
s_4												1	5	18	0	0	0	−2	−4	0	3	0	0	3	2	−4	95	1	5	16	6
s_5													−17	−2	7	0	0	−2	0	−3	1	0	0	1	−5	16	1	82	−17	−2	9
s_6														−4	−3	0	0	2	0	1	−3	0	0	3	9	10	6	−17	98	−2	−5
s_7															8	1	0	3	1	−1	−2	−3	0	−6	−1	13	18	−3	−4	84	5
s_8																0	0	−2	−1	−1	3	0	0	−5	−6	1	0	7	−2	6	19
c'_2																	1	−2	−3	−1	1	−4	−1	−2	1	0	0	0	0	1	0
c'_3																		−11	3	1	−1	−3	−2	0	−3	0	0	0	0	0	0
c'_4																			−1	−1	−1	−3	−1	−1	6	0	−1	−2	2	3	−2
c'_5																				−2	0	3	2	0	1	1	−4	0	0	1	−1
c'_6																					−4	0	0	1	−1	−1	0	−3	1	−1	0
c'_7																						−5	1	1	−5	−3	3	1	−3	−2	2
c'_8																							−2	0	0	0	0	0	0	−3	0
c'_9																								0	0	0	0	0	0	0	1
s'_1																									−2	−13	3	1	3	−8	9
s'_2																										−2	2	−5	9	−1	−8
s'_3																											−4	15	10	13	−4
s'_4																												0	5	16	6
s'_5																													−17	−2	7
s'_6																														−2	−5
s'_7																															3

Table 22. Correlation matrix (%) of statistical uncertainties for the modified optimal binning scheme with Δc_i and Δs_i constraints.

	c_2	c_3	c_4	c_5	c_6	c_7	c_8	s_1	s_2	s_3	s_4	s_5	s_6	s_7	s_8	c'_1	c'_2	c'_3	c'_4	c'_5	c'_6	c'_7	c'_8	s'_1	s'_2	s'_3	s'_4	s'_5	s'_6	s'_7	s'_8
c_1	80	74	22	−28	14	62	79	9	28	42	29	16	−20	−46	−46	76	67	69	5	−32	−1	56	69	−7	38	46	27	9	−20	−44	−48
c_2		71	23	−18	19	61	72	4	31	39	29	11	−15	−41	−38	55	87	63	11	−22	6	52	60	−2	39	43	27	4	−15	−39	−40
c_3			47	9	49	80	76	8	24	34	24	−4	−25	−31	−25	42	51	86	35	2	31	60	54	−1	40	43	20	−14	−25	−31	−35
c_4				66	68	47	33	1	−30	−46	−60	−16	36	26	12	−7	5	27	88	61	60	29	8	−23	−23	−40	−63	−22	36	27	4
c_5					61	15	−8	4	−37	−55	−54	−31	34	46	39	−53	−30	−7	70	98	64	2	−31	−10	−36	−51	−58	−33	34	47	36
c_6						52	30	3	−11	−21	−25	−23	16	20	22	−16	0	28	65	56	90	28	2	−2	0	−13	−30	−30	17	20	14
c_7							66	2	13	25	15	−14	−22	−31	−14	35	42	62	37	7	34	77	44	−5	32	34	12	−25	−21	−32	−28
c_8								11	22	32	20	7	−15	−33	−38	53	58	65	18	−14	13	51	83	−5	34	39	17	−2	−15	−32	−50
s_1									17	5	0	19	6	11	6	2	10	13	−3	5	5	1	7	17	9	5	−1	19	7	12	1
s_2										50	49	19	−40	−29	−15	26	24	31	−32	−37	−14	11	23	21	78	51	49	17	−40	−29	−17
s_3											84	−9	−73	−58	−39	46	43	47	−38	−55	−20	33	42	10	54	98	84	−11	−73	−57	−41
s_4												−7	−73	−55	−29	36	36	37	−47	−53	−23	23	31	12	52	82	99	−8	−73	−54	−32
s_5													35	11	8	14	9	−8	−41	−34	−40	−26	2	37	23	−6	−3	83	35	9	8
s_6														54	35	−29	−19	−38	18	33	9	−33	−28	13	−43	−70	−72	36	98	54	42
s_7															56	−51	−45	−44	19	46	17	−49	−48	27	−30	−55	−55	12	55	95	60
s_8																−49	−42	−42	4	36	14	−36	−57	39	−9	−33	−28	6	36	52	85
c'_2																	64	56	−11	−56	−19	46	69	−17	30	46	36	11	−30	−50	−49
c'_3																		59	3	−32	−2	48	62	−9	25	44	35	6	−20	−43	−41
c'_4																			31	−9	26	65	63	−14	35	48	33	−13	−38	−41	−47
c'_5																				69	72	34	5	−42	−33	−37	−52	−43	18	21	−0
c'_6																					63	−0	−33	−14	−42	−54	−57	−34	34	48	36
c'_7																						30	−0	−19	−16	−18	−28	−42	9	19	11
c'_8																							50	−26	16	33	20	−30	−33	−47	−41
c'_9																								−16	26	43	30	−1	−29	−46	−65
s'_1																									32	16	14	34	14	24	44
s'_2																										60	51	16	−42	−32	−17
s'_3																											82	−10	−70	−55	−38
s'_4																												−4	−71	−55	−31
s'_5																													35	11	10
s'_6																														54	43
s'_7																															58

Table 23. Correlation matrix (%) of systematic uncertainties for the equal binning scheme with Δc_i and Δs_i constraints.

	c_2	c_3	c_4	c_5	c_6	c_7	c_8	s_1	s_2	s_3	s_4	s_5	s_6	s_7	s_8	c'_1	c'_2	c'_3	c'_4	c'_5	c'_6	c'_7	c'_8	s'_1	s'_2	s'_3	s'_4	s'_5	s'_6	s'_7	s'_8
c_1	53	83	28	82	60	51	47	−13	4	−10	−11	22	9	32	−5	81	35	23	21	66	39	32	14	−14	3	−11	−14	19	15	36	−14
c_2		44	−10	36	44	52	37	−25	10	−12	−13	29	12	10	−23	42	88	21	−16	28	30	42	32	−26	7	−13	−15	28	17	17	−29
c_3			32	81	55	39	41	−7	11	−20	−3	16	6	33	2	60	26	26	26	56	34	17	1	−8	9	−21	−5	13	12	36	−5
c_4				58	6	−45	−16	53	−12	30	31	−40	−13	43	65	13	−19	−8	98	53	−6	−57	−58	53	−12	31	32	−43	−10	39	61
c_5					48	25	34	11	−6	6	5	−12	−2	45	26	62	20	15	53	82	28	4	−13	11	−8	5	4	−16	3	43	20
c_6						46	42	−18	11	−6	−6	28	33	25	−11	46	30	24	0	40	91	32	20	−19	10	−7	−8	26	38	29	−20
c_7							61	−49	7	−27	−24	49	19	2	−42	54	49	33	−47	25	43	94	58	−50	5	−29	−25	49	21	3	−49
c_8								−33	4	−13	−12	39	12	18	−25	46	33	20	−19	29	38	50	34	−33	4	−15	−13	38	14	20	−29
s_1									19	58	59	−61	−19	29	59	−32	−31	−19	51	−2	−26	−51	−45	98	23	59	61	−60	−18	35	60
s_2										10	7	12	7	6	−24	−7	4	−7	−14	−19	6	6	8	19	86	11	7	14	8	22	−25
s_3											45	−42	−21	21	45	−22	−16	−32	27	−9	−11	−30	−25	58	17	99	47	−42	−20	29	43
s_4												−39	−33	32	49	−32	−24	−16	24	−13	−16	−30	−31	59	10	47	89	−39	−30	34	63
s_5													39	−4	−56	31	30	21	−40	1	31	47	35	−60	11	−43	−40	99	39	0	−63
s_6														−12	−23	11	12	7	−12	2	29	18	14	−19	7	−21	−35	39	98	−10	−32
s_7															28	23	3	8	40	42	18	−13	−23	29	−1	18	34	−6	−10	78	35
s_8																−18	−28	−14	62	19	−18	−48	−41	59	−16	46	51	−58	−22	28	80
c'_2																	41	30	14	70	43	46	27	−33	−13	−26	−33	29	12	16	−26
c'_3																		21	−19	26	30	47	35	−31	−1	−18	−25	29	13	2	−33
c'_4																			−7	28	24	31	22	−19	−8	−34	−17	20	8	7	−19
c'_5																				54	−6	−56	−57	51	−16	27	26	−42	−11	32	58
c'_6																					36	14	−2	−3	−27	−12	−13	−2	3	30	12
c'_7																						38	26	−26	2	−13	−16	30	29	14	−25
c'_8																							66	−51	3	−32	−32	47	18	−15	−53
c'_9																								−45	6	−26	−32	36	14	−20	−45
s'_1																									23	60	61	−60	−18	34	60
s'_2																										19	10	14	10	28	−27
s'_3																											49	−43	−19	29	44
s'_4																												−40	−32	35	66
s'_5																													39	−0	−65
s'_6																														−5	−32
s'_7																															22

Table 24. Correlation matrix (%) of systematic uncertainties for the optimal binning scheme with Δc_i and Δs_i constraints.

	c_2	c_3	c_4	c_5	c_6	c_7	c_8	s_1	s_2	s_3	s_4	s_5	s_6	s_7	s_8	c'_1	c'_2	c'_3	c'_4	c'_5	c'_6	c'_7	c'_8	s'_1	s'_2	s'_3	s'_4	s'_5	s'_6	s'_7	s'_8
c_1	36	65	55	80	51	27	35	18	8	4	7	−7	−15	7	19	51	10	42	54	62	20	−2	−17	23	16	2	8	−11	−6	1	13
c_2		70	−15	42	66	70	60	−18	13	−29	−10	26	30	1	−23	40	80	47	−17	17	45	52	39	−14	27	−31	−6	27	39	7	−31
c_3			21	72	76	58	57	−8	11	−20	−4	15	16	6	−6	49	32	62	18	44	41	27	14	−1	29	−22	−1	16	27	11	−14
c_4				59	3	−35	−14	31	6	38	17	−30	−41	8	47	27	−32	10	99	67	−15	−51	−57	35	6	37	13	−36	−38	−3	47
c_5					55	31	36	22	−7	−4	14	−27	−22	2	23	47	13	46	57	79	21	−1	−15	28	2	−7	16	−30	−12	−7	20
c_6						64	64	−14	25	−19	−8	34	42	16	−27	50	46	59	3	37	86	42	26	−7	36	−22	−3	34	51	20	−33
c_7							70	−15	3	−47	−6	31	33	−1	−32	30	59	48	−36	1	48	70	49	−11	12	−48	0	33	41	2	−39
c_8								−23	15	−31	−13	39	34	6	−33	37	49	48	−14	14	49	51	37	−17	23	−33	−9	39	42	7	−33
s_1									−17	17	69	−63	−52	11	33	−18	−27	−19	30	8	−17	−38	−36	97	−19	19	70	−64	−52	3	49
s_2										33	−11	37	36	38	−34	22	7	12	7	−4	32	7	4	−12	90	31	−11	37	36	48	−31
s_3											29	−4	−16	21	32	−14	−38	−40	36	1	−15	−43	−33	16	32	93	24	−4	−21	27	37
s_4												−40	−45	26	42	−29	−25	−25	14	−8	−10	−30	−22	67	−10	30	86	−39	−46	24	55
s_5													60	14	−36	17	30	22	−29	−23	40	40	33	−59	39	−5	−39	98	62	23	−40
s_6														3	−63	21	35	22	−40	−21	47	45	39	−50	39	−17	−42	63	99	14	−67
s_7															−6	5	−4	1	8	−0	21	−10	−7	14	36	20	25	14	5	65	0
s_8																−23	−36	−24	45	19	−40	−43	−39	31	−33	34	38	−37	−65	−14	84
c'_2																	43	64	29	67	45	43	22	−11	24	−18	−27	13	30	−1	−27
c'_3																		47	−30	10	46	67	54	−24	9	−39	−20	30	40	−3	−42
c'_4																			11	48	50	45	29	−13	16	−43	−21	19	31	−4	−28
c'_5																				68	−14	−50	−57	33	5	35	10	−34	−37	−5	46
c'_6																					22	−2	−15	13	−3	−2	−7	−28	−13	−13	16
c'_7																						48	36	−13	33	−18	−5	39	52	25	−40
c'_8																							71	−36	9	−44	−25	41	49	−8	−50
c'_9																								−37	5	−34	−18	36	41	2	−41
s'_1																									−14	17	68	−61	−49	5	47
s'_2																										30	−10	40	41	51	−33
s'_3																											25	−6	−23	26	38
s'_4																												−38	−43	24	50
s'_5																													64	25	−43
s'_6																														15	−69
s'_7																															−9

Table 25. Correlation matrix (%) of systematic uncertainties for the modified optimal binning scheme with Δc_i and Δs_i constraints.

Data Availability Statement. This article has no associated data or the data will not be deposited.

Code Availability Statement. This article has no associated code or the code will not be deposited.

References

[1] N. Cabibbo, *Unitary Symmetry and Leptonic Decays*, *Phys. Rev. Lett.* **10** (1963) 531 [INSPIRE].

[2] M. Kobayashi and T. Maskawa, *CP Violation in the Renormalizable Theory of Weak Interaction*, *Prog. Theor. Phys.* **49** (1973) 652 [INSPIRE].

[3] J. Brod and J. Zupan, *The ultimate theoretical error on γ from $B \to DK$ decays*, *JHEP* **01** (2014) 051 [arXiv:1308.5663] [INSPIRE].

[4] CKMFitter Group, *CP violation and the CKM matrix: Assessing the impact of the asymmetric B factories*, *Eur. Phys. J. C* **41** (2005) 1 [hep-ph/0406184] [INSPIRE].

[5] H.-B. Li and X.-R. Lyu, *Study of the standard model with weak decays of charmed hadrons at BESIII*, *Natl. Sci. Rev.* **8** (2021) nwab181 [arXiv:2103.00908] [INSPIRE].

[6] A. Giri, Y. Grossman, A. Soffer and J. Zupan, *Determining gamma using $B^\pm \to DK^\pm$ with multibody D decays*, *Phys. Rev. D* **68** (2003) 054018 [hep-ph/0303187] [INSPIRE].

[7] A. Bondar, A. Poluektov and V. Vorobiev, *Charm mixing in the model-independent analysis of correlated $D^0\bar{D}^0$ decays*, *Phys. Rev. D* **82** (2010) 034033 [arXiv:1004.2350] [INSPIRE].

[8] M. Battaglieri et al., *Analysis Tools for Next-Generation Hadron Spectroscopy Experiments*, *Acta Phys. Pol. B* **46** (2015) 257 [arXiv:1412.6393] [INSPIRE].

[9] LHCb collaboration, *Measurement of the CKM angle γ in $B^\pm \to DK^\pm$ and $B^\pm \to D\pi^\pm$ decays with $D \to K^0_S h^+h^-$*, *JHEP* **02** (2021) 169 [arXiv:2010.08483] [INSPIRE].

[10] Belle collaboration, *Measurement of the CKM angle φ_1 in $B^0 \to \bar{D}^{(*)0}h^0$, $\bar{D}^0 \to K^0_S\pi^+\pi^-$ decays with time-dependent binned Dalitz plot analysis*, *Phys. Rev. D* **94** (2016) 052004 [arXiv:1607.05813] [INSPIRE].

[11] LHCb collaboration, *Observation of the Mass Difference Between Neutral Charm-Meson Eigenstates*, *Phys. Rev. Lett.* **127** (2021) 111801 [arXiv:2106.03744] [INSPIRE].

[12] BESIII collaboration, *Improved measurement of the strong-phase difference $\delta_D^{K\pi}$ in quantum-correlated $D\bar{D}$ decays*, *Eur. Phys. J. C* **82** (2022) 1009 [arXiv:2208.09402] [INSPIRE].

[13] CLEO collaboration, *Model-independent determination of the strong-phase difference between D^0 and $\bar{D}^0 \to K^0_{S,L}h^+h^-$ ($h = \pi, K$) and its impact on the measurement of the CKM angle γ/ϕ_3*, *Phys. Rev. D* **82** (2010) 112006 [arXiv:1010.2817] [INSPIRE].

[14] BESIII collaboration, *Model-independent determination of the relative strong-phase difference between D^0 and $\bar{D}^0 \to K^0_{S,L}\pi^+\pi^-$ and its impact on the measurement of the CKM angle γ/ϕ_3*, *Phys. Rev. D* **101** (2020) 112002 [arXiv:2003.00091] [INSPIRE].

[15] BESIII collaboration, *Measurement of integrated luminosity of data collected at 3.773 GeV by BESIII from 2021 to 2024*, *Chin. Phys. C* **48** (2024) 123001 [arXiv:2406.05827] [INSPIRE].

[16] BESIII collaboration, *Determination of U-spin breaking parameters with an amplitude analysis of the decay $D^0 \to K^0_L\pi^+\pi^-$*, arXiv:2212.09048 [INSPIRE].

JHEP06(2025)086

[17] Particle Data Group, *Review of particle physics*, *Phys. Rev. D* **110** (2024) 030001 [INSPIRE].

[18] BESIII collaboration, *Design and Construction of the BESIII Detector*, *Nucl. Instrum. Meth. A* **614** (2010) 345 [arXiv:0911.4960] [INSPIRE].

[19] C. Yu et al., *BEPCII Performance and Beam Dynamics Studies on Luminosity*, in the proceedings of the *7th International Particle Accelerator Conference*, Busan, South Korea, 8–13 May 2016 [DOI:10.18429/JACoW-IPAC2016-TUYA01] [INSPIRE].

[20] BESIII collaboration, *Future Physics Programme of BESIII*, *Chin. Phys. C* **44** (2020) 040001 [arXiv:1912.05983] [INSPIRE].

[21] J. Lu, Y. Xiao and X. Ji, *Online monitoring of the center-of-mass energy from real data at BESIII*, *Radiat. Detect. Technol. Meth.* **4** (2020) 337 [INSPIRE].

[22] J.-W. Zhang et al., *Suppression of top-up injection backgrounds with offline event filter in the BESIII experiment*, *Radiat. Detect. Technol. Meth.* **6** (2022) 289 [INSPIRE].

[23] Y.-X. Guo et al., *The study of time calibration for upgraded end cap TOF of BESIII*, *Radiat. Detect. Technol. Meth.* **1** (2017) 15 [INSPIRE].

[24] GEANT4 collaboration, *GEANT4 — A Simulation Toolkit*, *Nucl. Instrum. Meth. A* **506** (2003) 250 [INSPIRE].

[25] S. Jadach, B.F.L. Ward and Z. Was, *Coherent exclusive exponentiation for precision Monte Carlo calculations*, *Phys. Rev. D* **63** (2001) 113009 [hep-ph/0006359] [INSPIRE].

[26] S. Jadach, B.F.L. Ward and Z. Was, *The Precision Monte Carlo event generator $\kappa\kappa$ for two fermion final states in e^+e^- collisions*, *Comput. Phys. Commun.* **130** (2000) 260 [hep-ph/9912214] [INSPIRE].

[27] D.J. Lange, *The EvtGen particle decay simulation package*, *Nucl. Instrum. Meth. A* **462** (2001) 152 [INSPIRE].

[28] R.-G. Ping, *Event generators at BESIII*, *Chin. Phys. C* **32** (2008) 599 [INSPIRE].

[29] J.C. Chen, G.S. Huang, X.R. Qi, D.H. Zhang and Y.S. Zhu, *Event generator for J/ψ and $\psi(2S)$ decay*, *Phys. Rev. D* **62** (2000) 034003 [INSPIRE].

[30] R.-L. Yang, R.-G. Ping and H. Chen, *Tuning and Validation of the Lundcharm Model with J/ψ Decays*, *Chin. Phys. Lett.* **31** (2014) 061301 [INSPIRE].

[31] BESIII collaboration, *Amplitude analysis of the decays $D^0 \to \pi^+\pi^-\pi^+\pi^-$ and $D^0 \to \pi^+\pi^-\pi^0\pi^0$*, *Chin. Phys. C* **48** (2024) 083001 [arXiv:2312.02524] [INSPIRE].

[32] E. Barberio, B. van Eijk and Z. Was, *PHOTOS: A Universal Monte Carlo for QED radiative corrections in decays*, *Comput. Phys. Commun.* **66** (1991) 115 [INSPIRE].

[33] BaBar and Belle collaborations, *Measurement of $\cos 2\beta$ in $B^0 \to D^{(*)}h^0$ with $D \to K^0_S\pi^+\pi^-$ decays by a combined time-dependent Dalitz plot analysis of BaBar and Belle data*, *Phys. Rev. D* **98** (2018) 112012 [arXiv:1804.06153] [INSPIRE].

[34] ARGUS collaboration, *Search for Hadronic $b \to u$ Decays*, *Phys. Lett. B* **241** (1990) 278 [INSPIRE].

[35] BESIII collaboration, *Measurement of the $D \to K^-\pi^+\pi^+\pi^-$ and $D \to K^-\pi^+\pi^0$ coherence factors and average strong-phase differences in quantum-correlated $D\bar{D}$ decays*, *JHEP* **05** (2021) 164 [arXiv:2103.05988] [INSPIRE].

[36] A.J. Schwartz, *Effect of D^0-$\bar{D}^0$ Mixing upon Cabibbo-favored D^0 Decays*, arXiv:2207.11867 [INSPIRE].

[37] LHCb collaboration, *Physics case for an LHCb Upgrade II — Opportunities in flavour physics, and beyond, in the HL-LHC era*, arXiv:1808.08865 [INSPIRE].

[38] E. Kou et al., *The Belle II Physics Book*, *Prog. Theor. Exp. Phys.* **2019** (2019) 123C01 [*Erratum ibid.* **2020** (2020) 029201] [arXiv:1808.10567] [INSPIRE].

JHEP06(2025)086

The BESIII collaboration

M. Ablikim[1], M.N. Achasov[4,c], P. Adlarson[77], X.C. Ai[82], R. Aliberti[36], A. Amoroso[76A,76C], Q. An[73,59,a], Y. Bai[58], O. Bakina[37], Y. Ban[47,h], H.-R. Bao[65], V. Batozskaya[1,45], K. Begzsuren[33], N. Berger[36], M. Berlowski[45], M. Bertani[29A], D. Bettoni[30A], F. Bianchi[76A,76C], E. Bianco[76A,76C], A. Bortone[76A,76C], I. Boyko[37], R.A. Briere[5], A. Brueggemann[70], H. Cai[78], M.H. Cai[39,k,l], X. Cai[1,59], A. Calcaterra[29A], G.F. Cao[1,65], N. Cao[1,65], S.A. Cetin[63A], X.Y. Chai[47,h], J.F. Chang[1,59], G.R. Che[44], Y.Z. Che[1,59,65], C.H. Chen[9], Chao Chen[56], G. Chen[1], H.S. Chen[1,65], H.Y. Chen[21], M.L. Chen[1,59,65], S.J. Chen[43], S.L. Chen[46], S.M. Chen[62], T. Chen[1,65], X.R. Chen[32,65], X.T. Chen[1,65], X.Y. Chen[12,g], Y.B. Chen[1,59], Y.Q. Chen[35], Y.Q. Chen[16], Z.J. Chen[26,i], Z.K. Chen[60], S.K. Choi[10], X. Chu[12,g], G. Cibinetto[30A], F. Cossio[76C], J. Cottee-Meldrum[64], J.J. Cui[51], H.L. Dai[1,59], J.P. Dai[80], A. Dbeyssi[19], R.E. de Boer[3], D. Dedovich[37], C.Q. Deng[74], Z.Y. Deng[1], A. Denig[36], I. Denysenko[37], M. Destefanis[76A,76C], F. De Mori[76A,76C], B. Ding[68,1], X.X. Ding[47,h], Y. Ding[35], Y. Ding[41], Y.X. Ding[31], J. Dong[1,59], L.Y. Dong[1,65], M.Y. Dong[1,59,65], X. Dong[78], M.C. Du[1], S.X. Du[82], S.X. Du[12,g], Y.Y. Duan[56], P. Egorov[37,b], G.F. Fan[43], J.J. Fan[20], Y.H. Fan[46], J. Fang[60], J. Fang[1,59], S.S. Fang[1,65], W.X. Fang[1], Y.Q. Fang[1,59], R. Farinelli[30A], L. Fava[76B,76C], F. Feldbauer[3], G. Felici[29A], C.Q. Feng[73,59], J.H. Feng[16], L. Feng[39,k,l], Q.X. Feng[39,k,l], Y.T. Feng[73,59], M. Fritsch[3], C.D. Fu[1], J.L. Fu[65], Y.W. Fu[1,65], H. Gao[65], X.B. Gao[42], Y. Gao[73,59], Y.N. Gao[47,h], Y.N. Gao[20], Y.Y. Gao[31], S. Garbolino[76C], I. Garzia[30A,30B], P.T. Ge[20], Z.W. Ge[43], C. Geng[60], E.M. Gersabeck[69], A. Gilman[71], K. Goetzen[13], J.D. Gong[35], L. Gong[41], W.X. Gong[1,59], W. Gradl[36], S. Gramigna[30A,30B], M. Greco[76A,76C], M.H. Gu[1,59], Y.T. Gu[15], C.Y. Guan[1,65], A.Q. Guo[32], L.B. Guo[42], M.J. Guo[51], R.P. Guo[50], Y.P. Guo[12,g], A. Guskov[37,b], J. Gutierrez[28], K.L. Han[65], T.T. Han[1], F. Hanisch[3], K.D. Hao[73,59], X.Q. Hao[20], F.A. Harris[67], K.K. He[56], K.L. He[1,65], F.H. Heinsius[3], C.H. Heinz[36], Y.K. Heng[1,59,65], C. Herold[61], P.C. Hong[35], G.Y. Hou[1,65], X.T. Hou[1,65], Y.R. Hou[65], Z.L. Hou[1], H.M. Hu[1,65], J.F. Hu[57,j], Q.P. Hu[73,59], S.L. Hu[12,g], T. Hu[1,59,65], Y. Hu[1], Z.M. Hu[60], G.S. Huang[73,59], K.X. Huang[60], L.Q. Huang[32,65], P. Huang[43], X.T. Huang[51], Y.P. Huang[1], Y.S. Huang[60], T. Hussain[75], N. Hüsken[36], N. in der Wiesche[70], J. Jackson[28], Q. Ji[1], Q.P. Ji[20], W. Ji[1,65], X.B. Ji[1,65], X.L. Ji[1,59], Y.Y. Ji[51], Z.K. Jia[73,59], D. Jiang[1,65], H.B. Jiang[78], P.C. Jiang[47,h], S.J. Jiang[9], T.J. Jiang[17], X.S. Jiang[1,59,65], Y. Jiang[65], J.B. Jiao[51], J.K. Jiao[35], Z. Jiao[24], S. Jin[43], Y. Jin[68], M.Q. Jing[1,65], X.M. Jing[65], T. Johansson[77], S. Kabana[34], N. Kalantar-Nayestanaki[66], X.L. Kang[9], X.S. Kang[41], M. Kavatsyuk[66], B.C. Ke[82], V. Khachatryan[28], A. Khoukaz[70], R. Kiuchi[1], O.B. Kolcu[63A], B. Kopf[3], M. Kuessner[3], X. Kui[1,65], N. Kumar[27], A. Kupsc[45,77], W. Kühn[38], Q. Lan[74], W.N. Lan[20], T.T. Lei[73,59], M. Lellmann[36], T. Lenz[36], C. Li[48], C. Li[73,59], C. Li[44], C.H. Li[40], C.K. Li[21], D.M. Li[82], F. Li[1,59], G. Li[1], H.B. Li[1,65], H.J. Li[20], H.N. Li[57,j], Hui Li[44], J.R. Li[62], J.S. Li[60], K. Li[1], K.L. Li[20], K.L. Li[39,k,l], L.J. Li[1,65], Lei Li[49], M.H. Li[44], M.R. Li[1,65], P.L. Li[65], P.R. Li[39,k,l], Q.M. Li[1,65], Q.X. Li[51], R. Li[18,32], S.X. Li[12], T. Li[51], T.Y. Li[44], W.D. Li[1,65], W.G. Li[1,a], X. Li[1,65], X.H. Li[73,59], X.L. Li[51], X.Y. Li[1,8], X.Z. Li[60], Y. Li[20], Y.G. Li[47,h], Y.P. Li[35], Z.J. Li[60], Z.Y. Li[80], H. Liang[73,59], Y.F. Liang[55], Y.T. Liang[32,65], G.R. Liao[14], L.B. Liao[60], M.H. Liao[60], Y.P. Liao[1,65], J. Libby[27], A. Limphirat[61], C.C. Lin[56], D.X. Lin[32,65], L.Q. Lin[40], T. Lin[1], B.J. Liu[1], B.X. Liu[78], C. Liu[35], C.X. Liu[1], F. Liu[1], F.H. Liu[54], Feng Liu[6], G.M. Liu[57,j], H. Liu[39,k,l], H.B. Liu[15], H.H. Liu[1], H.M. Liu[1,65], Huihui Liu[22], J.B. Liu[73,59], J.J. Liu[21], K. Liu[39,k,l], K. Liu[74], K.Y. Liu[41], Ke Liu[23], L.C. Liu[44], Lu Liu[44], M.H. Liu[12,g], P.L. Liu[1], Q. Liu[65], S.B. Liu[73,59], T. Liu[12,g], W.K. Liu[44], W.M. Liu[73,59], W.T. Liu[40], X. Liu[39,k,l], X. Liu[40], X.K. Liu[39,k,l], X.Y. Liu[78], Y. Liu[82], Y. Liu[39,k,l], Y. Liu[82], Y.B. Liu[44], Z.A. Liu[1,59,65], Z.D. Liu[9], Z.Q. Liu[51], X.C. Lou[1,59,65], F.X. Lu[60],

JHEP06(2025)086

H.J. Lu[24], J.G. Lu[1,59], X.L. Lu[16], Y. Lu[7], Y.H. Lu[1,65], Y.P. Lu[1,59], Z.H. Lu[1,65], C.L. Luo[42], J.R. Luo[60], J.S. Luo[1,65], M.X. Luo[81], T. Luo[12,g], X.L. Luo[1,59], Z.Y. Lv[23], X.R. Lyu[65,p], Y.F. Lyu[44], Y.H. Lyu[82], F.C. Ma[41], H.L. Ma[1], J.L. Ma[1,65], L.L. Ma[51], L.R. Ma[68], Q.M. Ma[1], R.Q. Ma[1,65], R.Y. Ma[20], T. Ma[73,59], X.T. Ma[1,65], X.Y. Ma[1,59], Y.M. Ma[32], F.E. Maas[19], I. MacKay[71], M. Maggiora[76A,76C], S. Malde[71], Q.A. Malik[75], H.X. Mao[39,k,l], Y.J. Mao[47,h], Z.P. Mao[1], S. Marcello[76A,76C], A. Marshall[64], F.M. Melendi[30A,30B], Y.H. Meng[65], Z.X. Meng[68], G. Mezzadri[30A], H. Miao[1,65], T.J. Min[43], R.E. Mitchell[28], X.H. Mo[1,59,65], B. Moses[28], N.Yu. Muchnoi[4,c], J. Muskalla[36], Y. Nefedov[37], F. Nerling[19,e], L.S. Nie[21], I.B. Nikolaev[4,c], Z. Ning[1,59], S. Nisar[11,m], Q.L. Niu[39,k,l], W.D. Niu[12,g], C. Normand[64], S.L. Olsen[10,65], Q. Ouyang[1,59,65], S. Pacetti[29B,29C], X. Pan[56], Y. Pan[58], A. Pathak[10], Y.P. Pei[73,59], M. Pelizaeus[3], H.P. Peng[73,59], X.J. Peng[39,k,l], Y.Y. Peng[39,k,l], K. Peters[13,e], K. Petridis[64], J.L. Ping[42], R.G. Ping[1,65], S. Plura[36], V. Prasad[35], F.Z. Qi[1], H.R. Qi[62], M. Qi[43], S. Qian[1,59], W.B. Qian[65], C.F. Qiao[65], J.H. Qiao[20], J.J. Qin[74], J.L. Qin[56], L.Q. Qin[14], L.Y. Qin[73,59], P.B. Qin[74], X.P. Qin[12,g], X.S. Qin[51], Z.H. Qin[1,59], J.F. Qiu[1], Z.H. Qu[74], J. Rademacker[64], C.F. Redmer[36], A. Rivetti[76C], M. Rolo[76C], G. Rong[1,65], S.S. Rong[1,65], F. Rosini[29B,29C], Ch. Rosner[19], M.Q. Ruan[1,59], N. Salone[45], A. Sarantsev[37,d], Y. Schelhaas[36], K. Schoenning[77], M. Scodeggio[30A], K.Y. Shan[12,g], W. Shan[25], X.Y. Shan[73,59], Z.J. Shang[39,k,l], J.F. Shangguan[17], L.G. Shao[1,65], M. Shao[73,59], C.P. Shen[12,g], H.F. Shen[1,8], W.H. Shen[65], X.Y. Shen[1,65], B.A. Shi[65], H. Shi[73,59], J.L. Shi[12,g], J.Y. Shi[1], S.Y. Shi[74], X. Shi[1,59], H.L. Song[73,59], J.J. Song[20], T.Z. Song[60], W.M. Song[35], Y.J. Song[12,g], Y.X. Song[47,h,n], S. Sosio[76A,76C], S. Spataro[76A,76C], F. Stieler[36], S.S. Su[41], Y.J. Su[65], G.B. Sun[78], G.X. Sun[1], H. Sun[65], H.K. Sun[1], J.F. Sun[20], K. Sun[62], L. Sun[78], S.S. Sun[1,65], T. Sun[52,f], Y.C. Sun[78], Y.H. Sun[31], Y.J. Sun[73,59], Y.Z. Sun[1], Z.Q. Sun[1,65], Z.T. Sun[51], C.J. Tang[55], G.Y. Tang[1], J. Tang[60], J.J. Tang[73,59], L.F. Tang[40], Y.A. Tang[78], L.Y. Tao[74], M. Tat[71], J.X. Teng[73,59], J.Y. Tian[73,59], W.H. Tian[60], Y. Tian[32], Z.F. Tian[78], I. Uman[63B], B. Wang[60], B. Wang[1], Bo Wang[73,59], C. Wang[39,k,l], C. Wang[20], Cong Wang[23], D.Y. Wang[47,h], H.J. Wang[39,k,l], J.J. Wang[78], K. Wang[1,59], L.L. Wang[1], L.W. Wang[35], M. Wang[73,59], M. Wang[51], N.Y. Wang[65], S. Wang[12,g], T. Wang[12,g], T.J. Wang[44], W. Wang[60], W. Wang[74], W.P. Wang[36,59,73,o], X. Wang[47,h], X.F. Wang[39,k,l], X.J. Wang[40], X.L. Wang[12,g], X.N. Wang[1], Y. Wang[62], Y.D. Wang[46], Y.F. Wang[1,8,65], Y.H. Wang[39,k,l], Y.J. Wang[73,59], Y.L. Wang[20], Y.N. Wang[78], Y.Q. Wang[1], Yaqian Wang[18], Yi Wang[62], Yuan Wang[18,32], Z. Wang[1,59], Z.L. Wang[2], Z.L. Wang[74], Z.Q. Wang[12,g], Z.Y. Wang[1,65], D.H. Wei[14], H.R. Wei[44], F. Weidner[70], S.P. Wen[1], Y.R. Wen[40], U. Wiedner[3], G. Wilkinson[71], M. Wolke[77], C. Wu[40], J.F. Wu[1,8], L.H. Wu[1], L.J. Wu[1,65], L.J. Wu[20], Lianjie Wu[20], S.G. Wu[1,65], S.M. Wu[65], X. Wu[12,g], X.H. Wu[35], Y.J. Wu[32], Z. Wu[1,59], L. Xia[73,59], X.M. Xian[40], B.H. Xiang[1,65], D. Xiao[39,k,l], G.Y. Xiao[43], H. Xiao[74], Y.L. Xiao[12,g], Z.J. Xiao[42], C. Xie[43], K.J. Xie[1,65], X.H. Xie[47,h], Y. Xie[51], Y.G. Xie[1,59], Y.H. Xie[6], Z.P. Xie[73,59], T.Y. Xing[1,65], C.F. Xu[1,65], C.J. Xu[60], G.F. Xu[1], H.Y. Xu[68,2], H.Y. Xu[2], M. Xu[73,59], Q.J. Xu[17], Q.N. Xu[31], T.D. Xu[74], W. Xu[1], W.L. Xu[68], X.P. Xu[56], Y. Xu[41], Y. Xu[12,g], Y.C. Xu[79], Z.S. Xu[65], F. Yan[12,g], H.Y. Yan[40], L. Yan[12,g], W.B. Yan[73,59], W.C. Yan[82], W.H. Yan[6], W.P. Yan[20], X.Q. Yan[1,65], H.J. Yang[52,f], H.L. Yang[35], H.X. Yang[1], J.H. Yang[43], R.J. Yang[20], T. Yang[1], Y. Yang[12,g], Y.F. Yang[44], Y.H. Yang[43], Y.Q. Yang[9], Y.X. Yang[1,65], Y.Z. Yang[20], M. Ye[1,59], M.H. Ye[8,a], Z.J. Ye[57,j], Junhao Yin[44], Z.Y. You[60], B.X. Yu[1,59,65], C.X. Yu[44], G. Yu[13], J.S. Yu[26,i], L.Q. Yu[12,g], M.C. Yu[41], T. Yu[74], X.D. Yu[47,h], Y.C. Yu[82], C.Z. Yuan[1,65], H. Yuan[1,65], J. Yuan[35], J. Yuan[46], L. Yuan[2], S.C. Yuan[1,65], X.Q. Yuan[1], Y. Yuan[1,65], Z.Y. Yuan[60], C.X. Yue[40], Ying Yue[20], A.A. Zafar[75], S.H. Zeng[64,64,64,64], X. Zeng[12,g], Y. Zeng[26,i], Y.J. Zeng[60], Y.J. Zeng[1,65], X.Y. Zhai[35], Y.H. Zhan[60], A.Q. Zhang[1,65], B.L. Zhang[1,65], B.X. Zhang[1], D.H. Zhang[44], G.Y. Zhang[1,65],

JHEP06(2025)086

G.Y. Zhang[20], H. Zhang[73,59], H. Zhang[82], H.C. Zhang[1,59,65], H.H. Zhang[60], H.Q. Zhang[1,59,65], H.R. Zhang[73,59], H.Y. Zhang[1,59], J. Zhang[60], J. Zhang[82], J.J. Zhang[53], J.L. Zhang[21], J.Q. Zhang[42], J.S. Zhang[12,g], J.W. Zhang[1,59,65], J.X. Zhang[39,k,l], J.Y. Zhang[1], J.Z. Zhang[1,65], Jianyu Zhang[65], L.M. Zhang[62], Lei Zhang[43], N. Zhang[82], P. Zhang[1,8], Q. Zhang[20], Q.Y. Zhang[35], R.Y. Zhang[39,k,l], S.H. Zhang[1,65], Shulei Zhang[26,i], X.M. Zhang[1], X.Y. Zhang[41], X.Y. Zhang[51], Y. Zhang[74], Y. Zhang[1], Y.T. Zhang[82], Y.H. Zhang[1,59], Y.M. Zhang[40], Y.P. Zhang[73,59], Z.D. Zhang[1], Z.H. Zhang[1], Z.L. Zhang[35], Z.L. Zhang[56], Z.X. Zhang[20], Z.Y. Zhang[78], Z.Y. Zhang[44], Z.Z. Zhang[46], Zh.Zh. Zhang[20], G. Zhao[1], J.Y. Zhao[1,65], J.Z. Zhao[1,59], L. Zhao[73,59], L. Zhao[1], M.G. Zhao[44], N. Zhao[80], R.P. Zhao[65], S.J. Zhao[82], Y.B. Zhao[1,59], Y.L. Zhao[56], Y.X. Zhao[32,65], Z.G. Zhao[73,59], A. Zhemchugov[37,b], B. Zheng[74], B.M. Zheng[35], J.P. Zheng[1,59], W.J. Zheng[1,65], X.R. Zheng[20], Y.H. Zheng[65,p], B. Zhong[42], C. Zhong[20], H. Zhou[36,51,o], J.Q. Zhou[35], J.Y. Zhou[35], S. Zhou[6], X. Zhou[78], X.K. Zhou[6], X.R. Zhou[73,59], X.Y. Zhou[40], Y.X. Zhou[79], Y.Z. Zhou[12,g], A.N. Zhu[65], J. Zhu[44], K. Zhu[1], K.J. Zhu[1,59,65], K.S. Zhu[12,g], L. Zhu[35], L.X. Zhu[65], S.H. Zhu[72], T.J. Zhu[12,g], W.D. Zhu[12,g], W.D. Zhu[42], W.J. Zhu[1], W.Z. Zhu[20], Y.C. Zhu[73,59], Z.A. Zhu[1,65], X.Y. Zhuang[44], J.H. Zou[1], J. Zu[73,59]

[1] *Institute of High Energy Physics, Beijing 100049, People's Republic of China*
[2] *Beihang University, Beijing 100191, People's Republic of China*
[3] *Bochum Ruhr-University, D-44780 Bochum, Germany*
[4] *Budker Institute of Nuclear Physics SB RAS (BINP), Novosibirsk 630090, Russia*
[5] *Carnegie Mellon University, Pittsburgh, Pennsylvania 15213, USA*
[6] *Central China Normal University, Wuhan 430079, People's Republic of China*
[7] *Central South University, Changsha 410083, People's Republic of China*
[8] *China Center of Advanced Science and Technology, Beijing 100190, People's Republic of China*
[9] *China University of Geosciences, Wuhan 430074, People's Republic of China*
[10] *Chung-Ang University, Seoul, 06974, Republic of Korea*
[11] *COMSATS University Islamabad, Lahore Campus, Defence Road, Off Raiwind Road, 54000 Lahore, Pakistan*
[12] *Fudan University, Shanghai 200433, People's Republic of China*
[13] *GSI Helmholtzcentre for Heavy Ion Research GmbH, D-64291 Darmstadt, Germany*
[14] *Guangxi Normal University, Guilin 541004, People's Republic of China*
[15] *Guangxi University, Nanning 530004, People's Republic of China*
[16] *Guangxi University of Science and Technology, Liuzhou 545006, People's Republic of China*
[17] *Hangzhou Normal University, Hangzhou 310036, People's Republic of China*
[18] *Hebei University, Baoding 071002, People's Republic of China*
[19] *Helmholtz Institute Mainz, Staudinger Weg 18, D-55099 Mainz, Germany*
[20] *Henan Normal University, Xinxiang 453007, People's Republic of China*
[21] *Henan University, Kaifeng 475004, People's Republic of China*
[22] *Henan University of Science and Technology, Luoyang 471003, People's Republic of China*
[23] *Henan University of Technology, Zhengzhou 450001, People's Republic of China*
[24] *Huangshan College, Huangshan 245000, People's Republic of China*
[25] *Hunan Normal University, Changsha 410081, People's Republic of China*
[26] *Hunan University, Changsha 410082, People's Republic of China*
[27] *Indian Institute of Technology Madras, Chennai 600036, India*
[28] *Indiana University, Bloomington, Indiana 47405, USA*
[29] *INFN Laboratori Nazionali di Frascati , (A)INFN Laboratori Nazionali di Frascati, I-00044, Frascati, Italy; (B)INFN Sezione di Perugia, I-06100, Perugia, Italy; (C)University of Perugia, I-06100, Perugia, Italy*
[30] *INFN Sezione di Ferrara, (A)INFN Sezione di Ferrara, I-44122, Ferrara, Italy; (B)University of Ferrara, I-44122, Ferrara, Italy*

JHEP06(2025)086

[31] *Inner Mongolia University, Hohhot 010021, People's Republic of China*
[32] *Institute of Modern Physics, Lanzhou 730000, People's Republic of China*
[33] *Institute of Physics and Technology, Mongolian Academy of Sciences, Peace Avenue 54B, Ulaanbaatar 13330, Mongolia*
[34] *Instituto de Alta Investigación, Universidad de Tarapacá, Casilla 7D, Arica 1000000, Chile*
[35] *Jilin University, Changchun 130012, People's Republic of China*
[36] *Johannes Gutenberg University of Mainz, Johann-Joachim-Becher-Weg 45, D-55099 Mainz, Germany*
[37] *Joint Institute for Nuclear Research, 141980 Dubna, Moscow region, Russia*
[38] *Justus-Liebig-Universitaet Giessen, II. Physikalisches Institut, Heinrich-Buff-Ring 16, D-35392 Giessen, Germany*
[39] *Lanzhou University, Lanzhou 730000, People's Republic of China*
[40] *Liaoning Normal University, Dalian 116029, People's Republic of China*
[41] *Liaoning University, Shenyang 110036, People's Republic of China*
[42] *Nanjing Normal University, Nanjing 210023, People's Republic of China*
[43] *Nanjing University, Nanjing 210093, People's Republic of China*
[44] *Nankai University, Tianjin 300071, People's Republic of China*
[45] *National Centre for Nuclear Research, Warsaw 02-093, Poland*
[46] *North China Electric Power University, Beijing 102206, People's Republic of China*
[47] *Peking University, Beijing 100871, People's Republic of China*
[48] *Qufu Normal University, Qufu 273165, People's Republic of China*
[49] *Renmin University of China, Beijing 100872, People's Republic of China*
[50] *Shandong Normal University, Jinan 250014, People's Republic of China*
[51] *Shandong University, Jinan 250100, People's Republic of China*
[52] *Shanghai Jiao Tong University, Shanghai 200240, People's Republic of China*
[53] *Shanxi Normal University, Linfen 041004, People's Republic of China*
[54] *Shanxi University, Taiyuan 030006, People's Republic of China*
[55] *Sichuan University, Chengdu 610064, People's Republic of China*
[56] *Soochow University, Suzhou 215006, People's Republic of China*
[57] *South China Normal University, Guangzhou 510006, People's Republic of China*
[58] *Southeast University, Nanjing 211100, People's Republic of China*
[59] *State Key Laboratory of Particle Detection and Electronics, Beijing 100049, Hefei 230026, People's Republic of China*
[60] *Sun Yat-Sen University, Guangzhou 510275, People's Republic of China*
[61] *Suranaree University of Technology, University Avenue 111, Nakhon Ratchasima 30000, Thailand*
[62] *Tsinghua University, Beijing 100084, People's Republic of China*
[63] *Turkish Accelerator Center Particle Factory Group, (A)Istinye University, 34010, Istanbul, Turkey; (B)Near East University, Nicosia, North Cyprus, 99138, Mersin 10, Turkey*
[64] *University of Bristol, H H Wills Physics Laboratory, Tyndall Avenue, Bristol, BS8 1TL, UK*
[65] *University of Chinese Academy of Sciences, Beijing 100049, People's Republic of China*
[66] *University of Groningen, NL-9747 AA Groningen, The Netherlands*
[67] *University of Hawaii, Honolulu, Hawaii 96822, USA*
[68] *University of Jinan, Jinan 250022, People's Republic of China*
[69] *University of Manchester, Oxford Road, Manchester, M13 9PL, United Kingdom*
[70] *University of Muenster, Wilhelm-Klemm-Strasse 9, 48149 Muenster, Germany*
[71] *University of Oxford, Keble Road, Oxford OX13RH, United Kingdom*
[72] *University of Science and Technology Liaoning, Anshan 114051, People's Republic of China*
[73] *University of Science and Technology of China, Hefei 230026, People's Republic of China*
[74] *University of South China, Hengyang 421001, People's Republic of China*
[75] *University of the Punjab, Lahore-54590, Pakistan*
[76] *University of Turin and INFN, (A)University of Turin, I-10125, Turin, Italy; (B)University of Eastern Piedmont, I-15121, Alessandria, Italy; (C)INFN, I-10125, Turin, Italy*
[77] *Uppsala University, Box 516, SE-75120 Uppsala, Sweden*
[78] *Wuhan University, Wuhan 430072, People's Republic of China*

JHEP06(2025)086

[79] Yantai University, Yantai 264005, People's Republic of China
[80] Yunnan University, Kunming 650500, People's Republic of China
[81] Zhejiang University, Hangzhou 310027, People's Republic of China
[82] Zhengzhou University, Zhengzhou 450001, People's Republic of China

[a] Deceased
[b] Also at the Moscow Institute of Physics and Technology, Moscow 141700, Russia
[c] Also at the Novosibirsk State University, Novosibirsk, 630090, Russia
[d] Also at the NRC "Kurchatov Institute", PNPI, 188300, Gatchina, Russia
[e] Also at Goethe University Frankfurt, 60323 Frankfurt am Main, Germany
[f] Also at Key Laboratory for Particle Physics, Astrophysics and Cosmology, Ministry of Education; Shanghai Key Laboratory for Particle Physics and Cosmology; Institute of Nuclear and Particle Physics, Shanghai 200240, People's Republic of China
[g] Also at Key Laboratory of Nuclear Physics and Ion-beam Application (MOE) and Institute of Modern Physics, Fudan University, Shanghai 200443, People's Republic of China
[h] Also at State Key Laboratory of Nuclear Physics and Technology, Peking University, Beijing 100871, People's Republic of China
[i] Also at School of Physics and Electronics, Hunan University, Changsha 410082, China
[j] Also at Guangdong Provincial Key Laboratory of Nuclear Science, Institute of Quantum Matter, South China Normal University, Guangzhou 510006, China
[k] Also at MOE Frontiers Science Center for Rare Isotopes, Lanzhou University, Lanzhou 730000, People's Republic of China
[l] Also at Lanzhou Center for Theoretical Physics, Lanzhou University, Lanzhou 730000, People's Republic of China
[m] Also at the Department of Mathematical Sciences, IBA, Karachi 75270, Pakistan
[n] Also at Ecole Polytechnique Federale de Lausanne (EPFL), CH-1015 Lausanne, Switzerland
[o] Also at Helmholtz Institute Mainz, Staudinger Weg 18, D-55099 Mainz, Germany
[p] Also at Hangzhou Institute for Advanced Study, University of Chinese Academy of Sciences, Hangzhou 310024, China

JHEP06(2025)086